Economic Geology, v. 102, pp. 1415–1440

Fluid Evolution and Origins of Iron Oxide Cu-Au Prospects in the Olympic Dam District, Gawler Craton, South Australia

Evgeniy N. Bastrakov,† Roger G. Skirrow,

Geoscience Australia, GPO Box 378, Canberra, A.C.T., Australia 2601

and Garry J. Davidson

University of Tasmania, Private Box 79, Hobart, Tasmania, Australia 7001

Abstract

Geologic observations suggest two stages of hydrothermal activity at a number of presently subeconomic iron oxide copper-gold systems in the Olympic Dam district, eastern Gawler craton. They contain high-, and moderate- to low-temperature Fe oxide-rich hydrothermal alteration. The mineral assemblages include magnetite-calc-silicate-alkali feldspar ± Fe-Cu sulfides and hematite-sericite-chlorite-carbonate ± Fe-Cu sulfides ± U, REE minerals. In all documented prospects, the minerals of the hematitic assemblages replace the minerals of the magnetite-rich assemblages.

The bulk of the subeconomic Cu-Au mineralization is associated with the hematitic alteration assemblages. Microanalysis by proton ion probe (PIXE) of hypersaline fluid inclusions in magnetite-rich assemblages, however, demonstrates that significant amounts of copper (>500 ppm) were transported by the early-stage high-temperature (>400°C) fluids responsible for the magnetite-rich alteration. These brine inclusions contain multiple solid phases (liquid + vapor + multiple solids) including chalcopyrite in some cases. In comparison, inclusions of the hematitic stage are relatively simple liquid + vapor types, with homogenization temperatures of 200° to 300°C and containing 1 to 8 wt percent NaCl equiv. The Br/Cl ratios of the magnetite-forming fluids measured by PIXE lie beyond the range of typical magmatic and/or mantle values, allowing for the possibility that the fluids originated as brines from a sedimentary basin or the crystalline basement.

Sulfur isotope compositions of chalcopyrite and pyrite demonstrate that sulfur in both alteration assemblages was derived either from cooling magmas and/or crystalline igneous rocks carried by relatively oxidized fluids ($\Sigma SO_4^{2-} \approx \Sigma H_2S$, $\delta^{34}S_{sulfides}$ from –5 to +2‰) or from crustal sedimentary rocks ($\delta^{34}S_{sulfides}$ from +5 to +10‰). Oxygen and hydrogen isotope compositions of waters calculated for minerals of the magnetite-rich assemblage have $\delta^{18}O$ values of +7.7 to +12.8 per mil and δD values of –15 to –21 per mil. The only available $\delta^{18}O$ and δD_{fluid} values for the hematitic assemblage are +4.7 and –9 per mil, respectively. The isotopic compositions of both fluids, coupled with the available literature data, can be explained in terms of fluid reequilibration with felsic Gawler Range Volcanics or other felsic igneous rocks in the region and with metasedimentary rocks of the Wallaroo Group at low water-to-rock ratios prior to their arrival at the mineralization sites.

The lack of significant copper mineralization associated with magnetite-forming fluids that carried copper suggests that there was no effective mechanism of saturation of copper minerals or the quantity of these fluids was not sufficient to produce appreciable copper mineralization. Association of the copper-gold mineralization with the hematitic alteration in the subeconomic prospects can be explained by a two-stage model in which preexisting hydrothermal magnetite with minor associated copper-gold mineralization was flushed by late-stage oxidized brines that had extensively reacted with sedimentary or metamorphic rocks. The reduction of these brines, driven by conversion of magnetite to hematite, resulted in precipitation of copper and gold. The oxidized brines may have contributed additional copper and gold to the system in addition to upgrading preexisting subeconomic Cu-Au mineralization. When compared to published models for the Olympic Dam deposit, the new data for fluids in subeconomic Fe-oxide Cu-Au prospects of the Olympic Dam district indicate the diversity of origins of iron oxide-copper-gold systems, even within the same geologic region.

Introduction

In his review of iron oxide copper-gold (IOCG) deposits, Hitzman (2000) noted that a comprehensive genetic model that can help distinguish productive from barren or subeconomic systems is still lacking. Although IOCG deposits globally share many features, such as abundant Fe oxides (magnetite or hematite) and widespread sodic-calcic, potassic or hydrolytic alteration (Hitzman et al., 1992; Hitzman, 2000), the family of IOCG deposits is very diverse. Many IOCG districts also contain magnetite-apatite deposits of so-called Kiruna type, but no set of geologic features distinguishes economic Cu-Au systems from these large accumulations of Fe oxides containing only anomalous amounts of these metals (Barton and Johnson, 2004). They speculated whether this contrast in ore metal abundance reflects fundamental differences in the genesis of these hydrothermal systems or the lack of efficient traps or metal sources. The iron oxides may have formed concurrently with Cu-Au mineralization (e.g., Haynes et al., 1995) or may have largely predated the introduction of the ore metals (e.g., Skirrow, 2000).

The eastern Gawler craton, South Australia (Fig. 1), is host to the 3.81 billion metric ton (Gt) Olympic Dam Cu-U-Au-Ag-REE deposit (Reeve et al., 1990) and the recently discovered Prominent Hill Cu-Au deposit (Belperio, 2002). Numerous subeconomic Fe oxide-rich hydrothermal alteration

† Corresponding author: e-mail, evgeniy.bastrakov@ga.gov.au

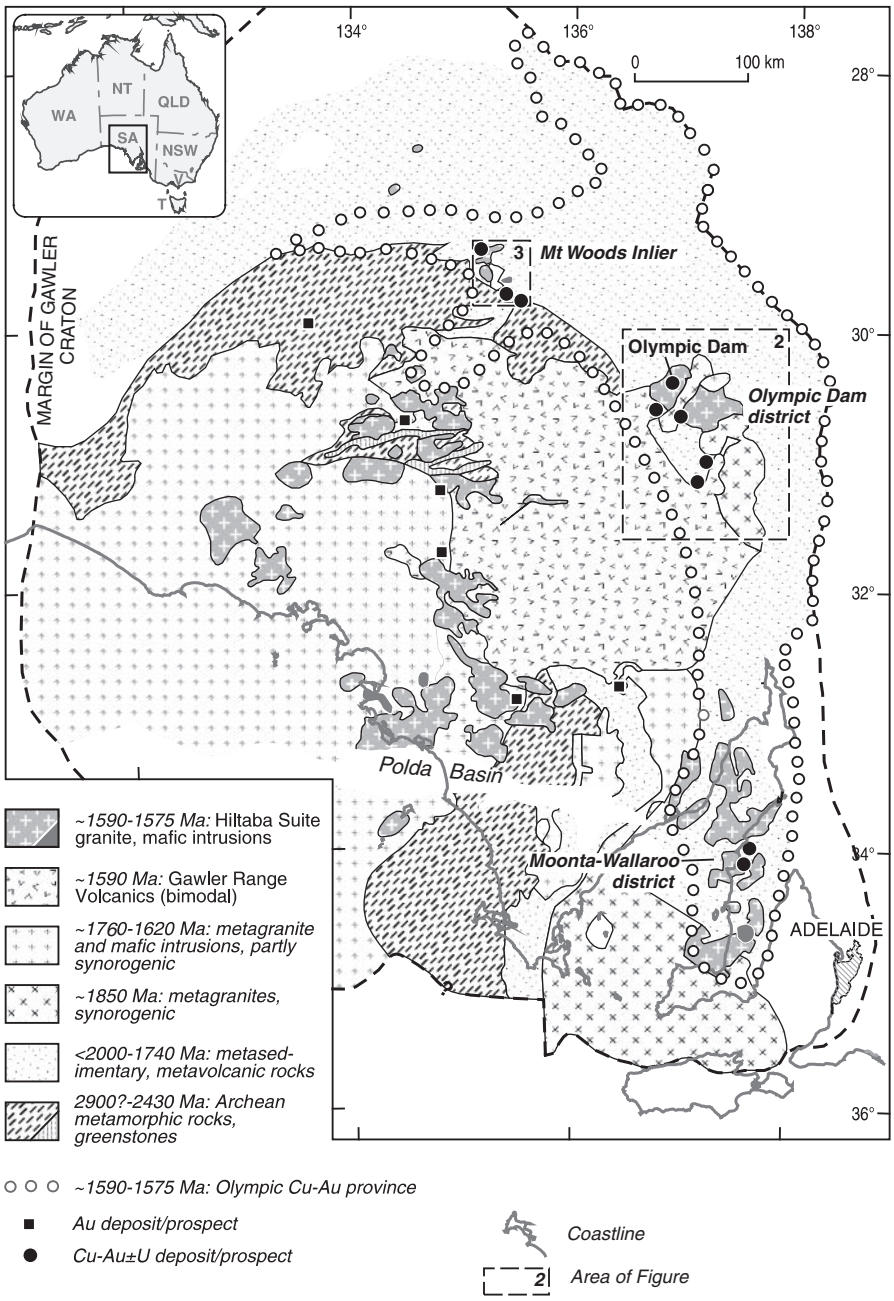

FIG. 1. Location and simplified geology of the Gawler craton (Skirrow et al., 2007), showing the Olympic Cu-Au province (Skirrow et al., 2002) and major Cu-Au and Au deposits and prospects. The two boxes correspond to Figures 2 and 3. The Polda basin (Neoproterozoic to Mesozoic) overlies the Archean-Mesozoic basement.

systems are also known from the eastern Gawler craton, within the Olympic Cu-Au province (Skirrow et al., 2002).

For mineral explorers, an additional challenge is in discriminating between major mineralized IOCG systems and subeconomic or minor systems concealed by deep cover, where minimal geologic and geochemical data are available. The lack of comprehensive information published on the numerous IOCG alteration systems elsewhere in the Olympic Cu-Au province adds to this challenge. The present contribution aims to provide a mineralogical, geochemical, and fluid evolution context for understanding the relationships between subeconomic IOCG prospects and the major economic IOCG deposits in the Olympic Cu-Au province.

Previous Work and Scope of the Present Study

The main focus of previously published descriptions and research within the Olympic Cu-Au province has been the Olympic Dam deposit itself (e.g., Oreskes and Einaudi, 1990, 1992; Reeve et al., 1990; Haynes et al., 1995; Johnson and Cross, 1995; Johnson and McCulloch, 1995; Reynolds, 2000, 2001) and Cu-Au vein deposits in the Moonta-Wallaroo district (Conor, 1995; Morales et al., 2002). Few studies have

documented in detail the geology, hydrothermal alteration, and mineralization of the many IOCG prospects in the Olympic Dam district or in the Olympic Cu-Au province as a whole (Figs. 1, 2). Valuable information is available from company reports (e.g., Paterson and Muir, 1986; Curtis et al., 1993), and summary descriptions of the Acropolis and Wirrda Well prospects are given in Drexel et al. (1993). Gow et al. (1994) and Gow (1996) considered in detail the hydrothermal system at Emmie Bluff, including oxygen isotope fingerprinting of ore fluids. Knutson et al. (1992) studied alteration patterns of the Gawler Range Volcanics in the Mount Gunson area and reported results of petrological, fluid inclusion, and

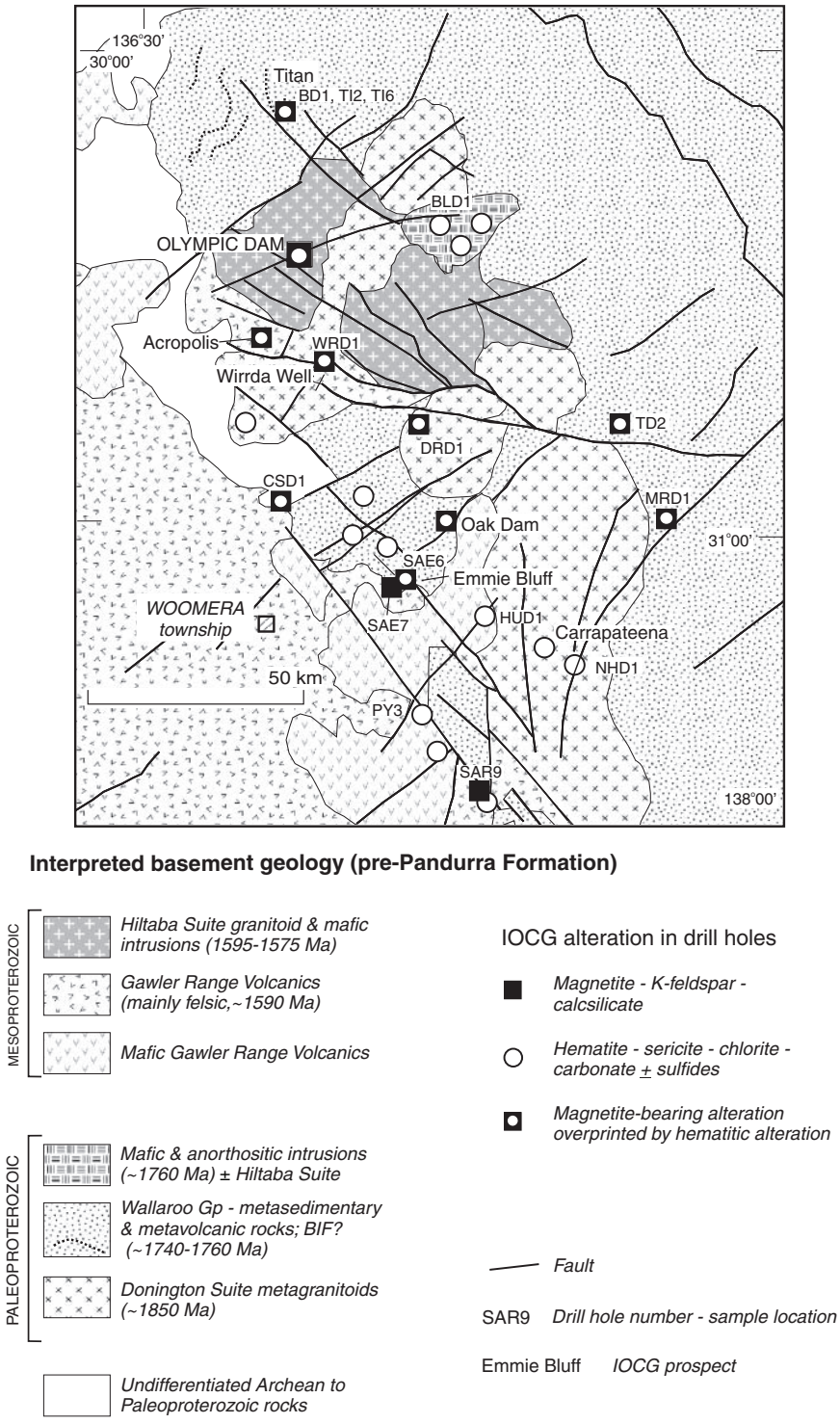

FIG. 2. Interpreted pre-Neoproterozoic basement geology and IOCG hydrothermal alteration in the Olympic Dam district of the Olympic Cu-Au province. See Figure 1 for location.

stable isotope (S, C, and O) studies. Davidson and Paterson (1993) summarized a study of the Oak Dam deposit, reported in detail in 2007 (Davidson et al., 2007). In the Mount Woods inlier, Hampton (1997) described the Manxman and Joes Dam IOCG prospects, whereas only summary information has been available on the Prominent Hill deposit (Belperio, 2002). The Moonta-Wallaroo Cu-Au district has received more attention (e.g., Conor, 1995; Morales et al., 2002). Based on new geologic and petrological observations and on compilation of the available literature data, Skirrow et al. (2002) provided a summary of characteristics of hydrothermal IOCG alteration and mineralization in the Olympic Cu-Au province.

The current paper updates the descriptions presented by Skirrow et al. (2002) and focuses on the Olympic Dam district, one of the world's most important IOCG districts. We report fluid inclusion and stable isotope data and consider the evolution and sources of fluids responsible for alteration and mineralization in a number of subeconomic IOCG systems in the region and the implications of these results for models of Cu-Au mineralization.

Regional Geologic Setting

The geology of the Olympic Dam district (Fig. 2) is briefly described below. For details, the reader is referred to Direen and Lyons (2007), Hand et al. (2007), and Skirrow et al. (2007).

Mesoproterozoic and older crystalline basement of the Olympic Dam district (Fig. 2) is covered by >200 m (commonly >500 m) of Neoproterozoic, Cambrian, and younger sedimentary basin rocks, collectively known as the Stuart Shelf. The principal basement units are interpreted from potential field data and relatively sparse drilling (Direen and Lyons, 2002, 2007). The oldest known lithologic units are voluminous, intensely deformed syntectonic granitoids of the Donington Suite, emplaced between 1850 ± 3.5 and 1860 ± 4 Ma (Jagodzinski, 2005). Older Paleoproterozoic metasedimentary rocks and Archean crust have not been directly observed in the region but are inferred from geophysical modeling (Direen and Lyons, 2007). Large areas of basement are inferred to comprise the Wallaroo Group, a compositionally diverse package of metasedimentary rocks deposited between ~1740 and ~1760 Ma (Jagodzinski, 2005). This group comprises thin-bedded feldspathic to biotite-rich metasiltstones, metacarbonate rocks, minor banded iron formation, and rare carbonaceous metapelitic rocks. Underlying these rocks are red K-feldspar-bearing meta-arkosic rocks, with maximum depositional ages of ~1850 to 1855 Ma (Jagodzinski, 2005). They may represent the lower part of the Wallaroo Group or a separate older unit. The only igneous rocks of possibly Wallaroo Group age identified in the Olympic Dam district are leucogabbros in the Bills Lookout area (e.g., drill holes BLD1, BLD2, Fig. 2), which contain zircons with an age of 1764 ± 12 Ma (Johnson, 1993). The age of metamorphism and deformation of the Paleoproterozoic rocks is poorly constrained in the Olympic Dam district but may correspond to the Kimban orogeny, the effects of which were widespread elsewhere in the eastern Gawler craton about ~1700 to 1730 Ma (Daly et al., 1998).

The Paleoproterozoic basement in the Olympic Dam district was unconformably overlain by generally flat-lying and essentially unmetamorphosed units of the Gawler Range Volcanics, a large-volume, felsic-dominated bimodal igneous province (Drexel et al., 1993). In the Olympic Dam district the only published U-Pb zircon determination for the Gawler Range Volcanics is 1591 ± 10 Ma from the Wirrda Well prospect (Fig. 2; Creaser and Cooper, 1993). The Gawler Range Volcanics was comagmatic with the Hiltaba Suite, which comprises granites, granodiorites, quartz monzonites, quartz syenite, and quartz monzodiorites (Drexel et al., 1993). The Hiltaba Suite is widespread throughout the central and eastern Gawler craton including the Olympic Dam district, where it hosts the Olympic Dam deposit. The most precise zircon U-Pb ages for Hiltaba Suite granitoids in this district cluster around 1588 to 1596 Ma (Mortimer et al., 1988; Creaser and Cooper, 1993; Johnson and Cross, 1995; Jagodzinski, 2005). Mafic intrusions of comparable age have been increasingly recognized in the Olympic Dam district (Johnson and Cross, 1995; Jagodzinski, 2005), as well as in each of the other two main IOCG districts of the Olympic Cu-Au province (Skirrow et al., 2007). The nature of deformation in the early Mesoproterozoic, during IOCG formation, has been characterized by Direen and Lyons (2007), and Hand et al. (2007). Deformation of the Hiltaba Suite granites and Gawler Range Volcanics in the Olympic Dam district appears to have been restricted to local brittle-style fracturing, brecciation, and faulting.

Alteration and Mineralization

Taking into account the absence of outcrop in the studied area, documentation and mapping of alteration in this study were based on the examination of drill core (App. 1). The drill holes selected for detailed examination were initially screened using the drill hole logs published by the Department of Primary Industries and Resources of South Australia (PIRSA; Curtis et al., 1993). Drill holes were examined in the PIRSA core library in Adelaide and sampled for petrographic work and fluid inclusion analysis (Conventional micothermometry and proton induced X-ray emission), and stable (S, O, H) and radiogenic (Sm-Nd, ^{39}Ar-^{40}Ar, Re-Os) isotope studies (see Skirrow et al., 2007). This sample set was supplemented with proprietary drill core from the Titan prospect (Fig. 2) provided by Tasman Resources.

The main challenge in understanding the spatial distribution of the alteration types is correlating alteration assemblages intersected in widely separated diamond drill holes dispersed over a distance of 200 km (Fig. 2). Historically, most of the drilling targeted geophysical anomalies with coincident magnetic and gravity anomalies resulting from magnetite-rich hydrothermal alteration. Recent discoveries of hematite-dominated IOCG systems characterized by gravity highs with little or no magnetic response (e.g., Prominent Hill and Carrapateena) mean that many of the drill holes in the present study were biased toward magnetite-bearing alteration.

Alteration types and paragenesis

The key hydrothermal alteration and ore mineral assemblages recognized in the Olympic Dam district are magnetite-alkali feldspar-calc-silicate ± Fe-Cu sulfides and hematite-sericite-chlorite-carbonate ± Fe-Cu sulfides ± U and REE minerals (abbreviated to "hematitic alteration"). The magnetite-biotite alteration assemblage observed in other parts of

the Olympic Cu-Au province (Skirrow et al., 2002) has not been recognized in the Olympic Dam district. All three alteration assemblages occur as veins and replacements of host rocks ranging from felsic to mafic in composition.

The magnetite-feldspar-calc-silicate assemblage is further subdivided into two types: magnetite-albite-calc-silicate (Fe-Na-Ca–rich) alteration and a K-rich alteration in which K-feldspar replaced albite. This magnetite-K-feldspar-calc-silicate assemblage is by far the dominant magnetite-bearing assemblage in the IOCG systems studied. The calc-silicates are generally actinolite or diopside; minerals present in both magnetite-bearing assemblages in minor to trace abundances are quartz, pyrite, apatite, titanite, chalcopyrite, scapolite, and allanite.

The regional distribution and local temporal relationships between magnetite-bearing and hematitic alteration are summarized in Figures 2 and 3. In many examined drill holes (Figs. 2–4, App. 1), both assemblages are present, with hematitic assemblages replacing preexisting magnetite-bearing assemblages to different degrees. Nevertheless, it is possible to

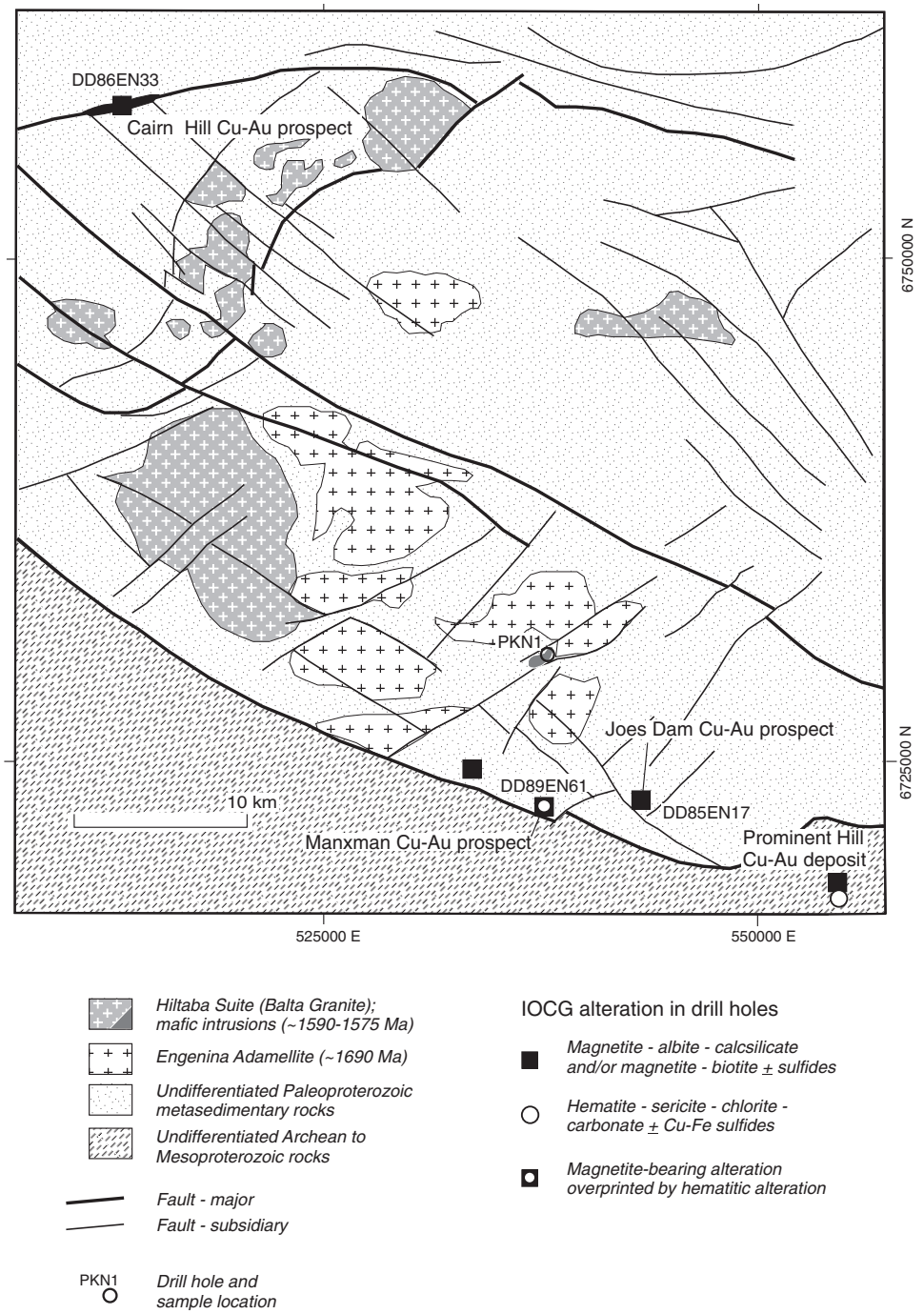

FIG. 3. Interpreted pre-Neoproterozoic basement geology and IOCG hydrothermal alteration of part of the Mount Woods inlier of the Olympic Cu-Au province. Modified and simplified from Betts et al. (2003). See Figure 1 for location.

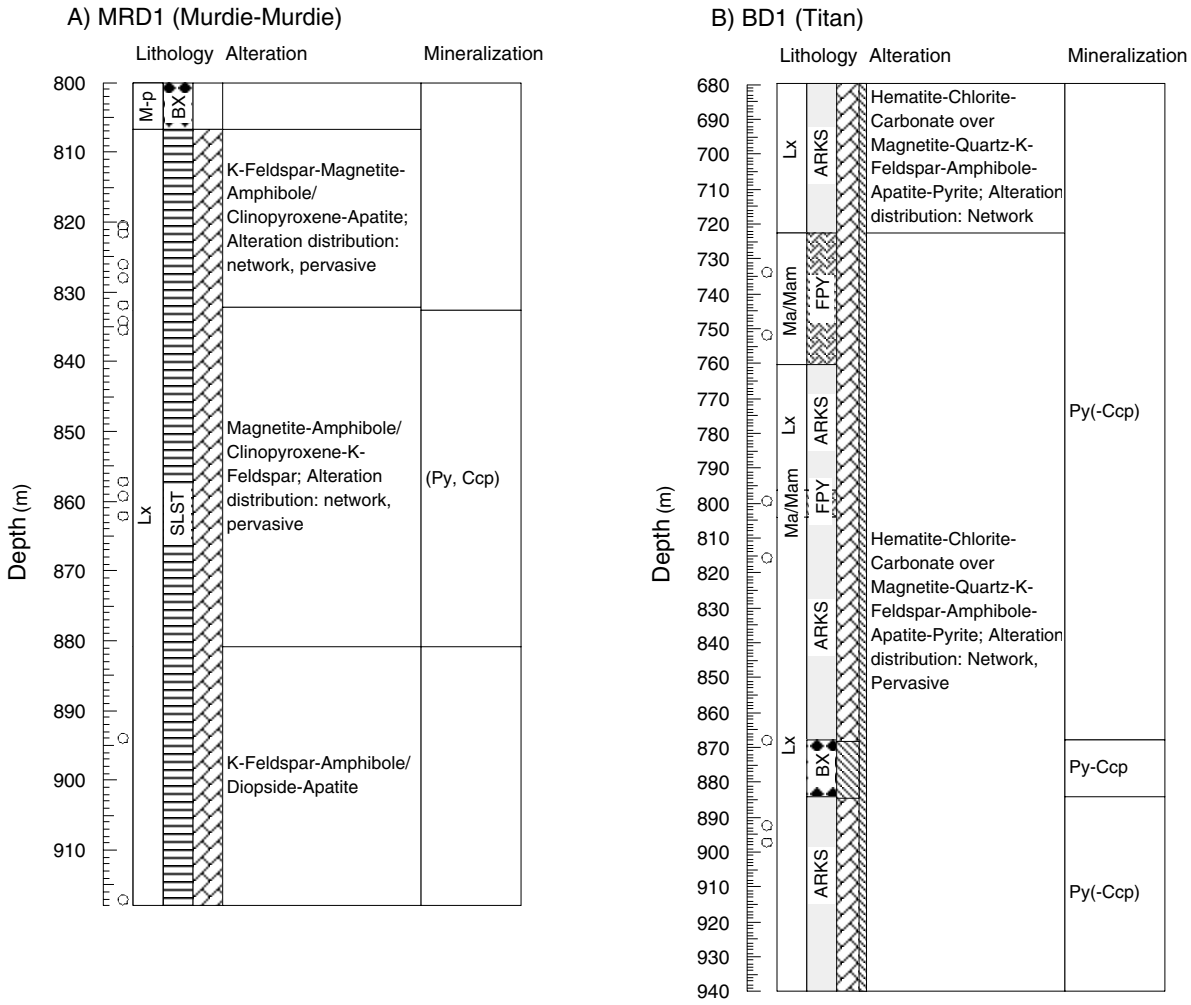

FIG. 4. Reference IOCG alteration types in the Olympic Dam district, based on the drill logs from the Murdie-Murdie (A), Titan (B), Emmie Bluff (C), and Torrens prospects (D). (A) and (B). Drill holes dominated by high-temperature magnetite-K-feldspar-calc-silicate alteration. (C) and (D). Medium- to low-temperature hematite-sericite-chlorite-carbonate alteration superimposed on magnetite-bearing alteration. Lithostratigraphic units: Lx = Wallaroo Group, M-p = Pandurra Formation, Ma/Mam = interdigitated felsic and mafic Gawler Range Volcanics, Ppd = Donington Granitoid Suite. Lithologic units: ARKS = arkose; BX = breccia; CNGL = conglomerate; FPY = felsic porphyry dike, GRT = granite, SLST = siltstone. Mineral abbreviations: Bn = bornite; Ccp = chalcopyrite; Cv = covellite; Py = pyrite. Brackets denote minerals in minor and/or trace abundances.

sample drill holes and hydrothermal systems where the end-member alteration types are represented quite distinctly—for example, at Murdie Murdie and Titan (magnetite-K-feldspar-calc-silicate alteration) and Emmie Bluff and Torrens (hematite-sericite-chlorite-carbonate alteration; Figs. 2, 4). Typical altered rocks, ore mineral assemblages, and some paragenetic relationships are shown in Figure 5. For details of the key geologic and mineralogical features of the studied prospects the reader is referred to table 1 of Skirrow et al. (2007).

Murdie Murdie

The hydrothermal system at Murdie Murdie is located approximately 7 km east of the southern end of Andamooka Island in Lake Torrens (Fig. 2). Drill hole MRD1 targeted coincident magnetic and gravity anomalies (Paterson and Muir, 1986) resulting from the magnetite-bearing alteration (Fig. 2). This drill hole contains the least intense overprint by the hematitic assemblage and is used here to represent end-member magnetite-K-feldspar-calc-silicate alteration (Figs. 4, 5A-F). The drill hole is characterized by abundant magnetite, developed as replacement zones and veins within altered fine-grained quartzofeldspathic metasedimentary rock. Magnetite is accompanied by hematite-stained red feldspar (K-feldspar + albite), actinolite, apatite, titanite, pyrite, and traces of chalcopyrite (Fig. 5A-E). The prominent feature of this drill hole is a zone of coarse-grained, subhedral magnetite associated with pink centimeter-scale subhedral microcline that replaced albite and coarse-grained pink apatite (Fig. 5A). Carbonate, quartz, pyrite, and chalcopyrite are interstitial to these minerals; some quartz and carbonate infill fractures in the coarse-grained minerals (Fig. 5C-E). As noted by Paterson and Muir (1986), the coarse-grained magnetite-rich zone may represent either total replacement of

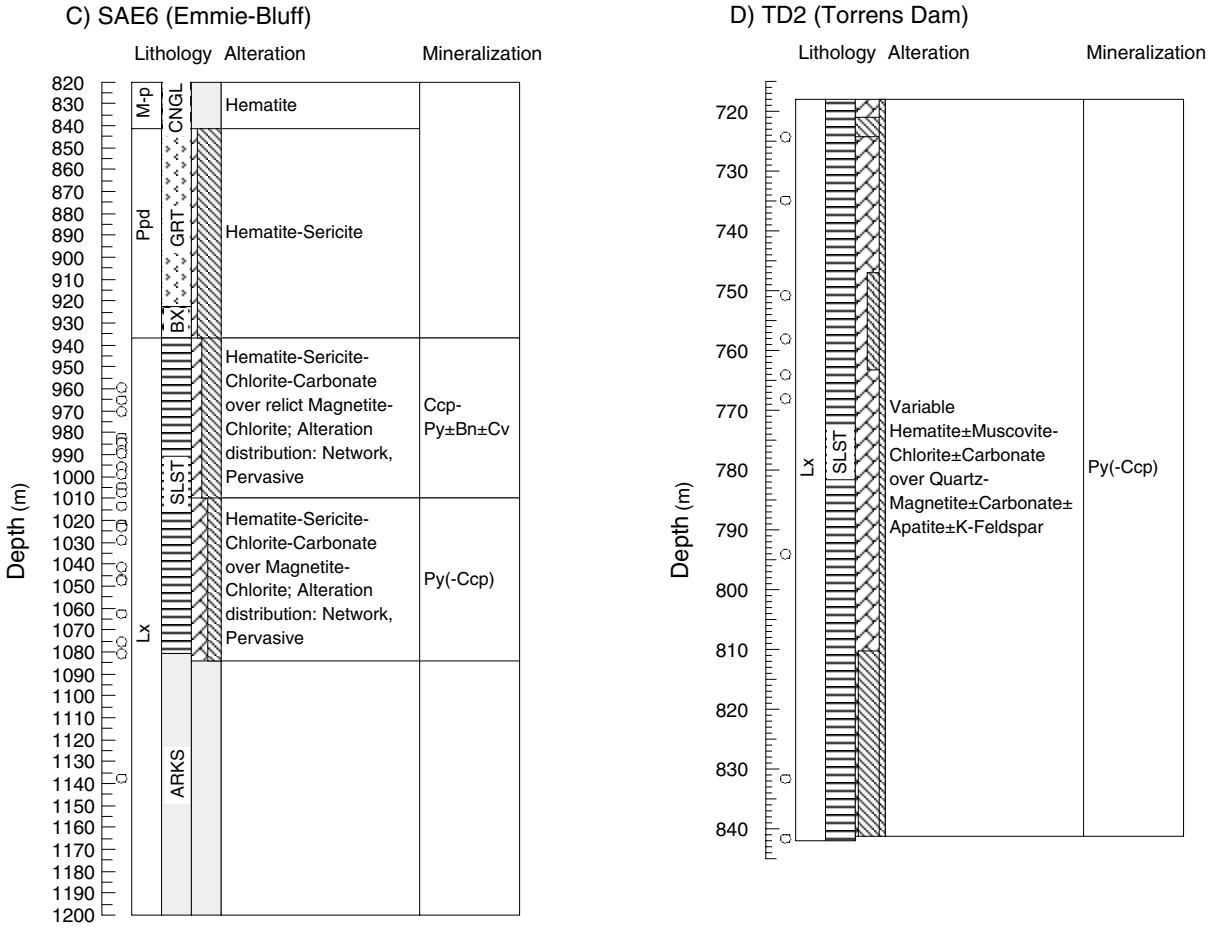

FIG. 4. *(Cont.)*

the host metasedimentary rock or a zone of strong veining. Dating of hydrothermal titanite in this alteration by the SHRIMP U-Pb method yielded an age of 1576 ± 5 Ma, interpreted as the age of magnetite-bearing hydrothermal alteration at Murdie Murdie (Skirrow et al., 2007).

Later alteration is represented by partial martitization of magnetite (Fig. 5E), chloritization of amphibole, and deposition of calcite. The extent of this hematite-chlorite-carbonate assemblage within drill hole MRD1 is extremely limited.

There are no significant assays associated with the alteration within drill hole MRD1, but the magnetite-enriched zone shows weak enrichment in copper (30–120 ppm: Paterson and Muir, 1986).

Titan

The Titan prospect is another example of an IOCG system dominated by magnetite-K-feldspar-calc-silicate alteration, with minor hematitic alteration. This prospect is situated ~25 km north-northeast of the Olympic Dam deposit (Fig. 2). Hydrothermal alteration and sulfide mineralization are hosted mainly by meta-arkose. Alteration is also hosted by thin-bedded feldspathic to carbonaceous and biotite-rich metasiltstone, similar to that in the upper Wallaroo Group farther south, and by unmetamorphosed felsic porphyry dikes similar to Gawler Range Volcanics. The metasiltstones are steeply dipping with a strong shear foliation developed subparallel to compositional layering. Fine-grained mafic dikes up to 30 m thick, but typically <2 m thick, occur in several holes including the two selected for more detailed study (BD1, Fig. 4; TI2). These dikes are of particular interest because they are intimately associated with late-stage brecciation and hematitic alteration, as described below.

Titan is characterized by long intervals of subeconomic sulfide mineralization with 0.1 to 0.2 wt percent Cu. The best intersection is 5 m at 1.14 wt percent Cu (Tasman Resources, 2004 Annual Report).

Hydrothermal alteration overprints the shear foliation in the thin-bedded metasedimentary units, and alteration appears to locally penetrate along the foliation and compositional layering. Drill holes BD1 and TI2 intersected altered meta-arkose, felsic and mafic dikes and breccia zones (Fig. 5A). Magnetite-K-feldspar-calc-silicate and hematitic alteration assemblages are well zoned in drill hole TI2. The upper and lower parts of drill hole TI2 and much of BD1 are dominated by magnetite-K-feldspar-calc-silicate assemblages, comprising vein and replacement networks of magnetite, quartz, actinolite or tremolite, pyrite, hematite-dusted K-feldspar, and minor chalcopyrite. Rare examples of coarse-bladed magnetite-hematite intergrowths indicate that conditions were close to hematite-magnetite equilibrium prior to

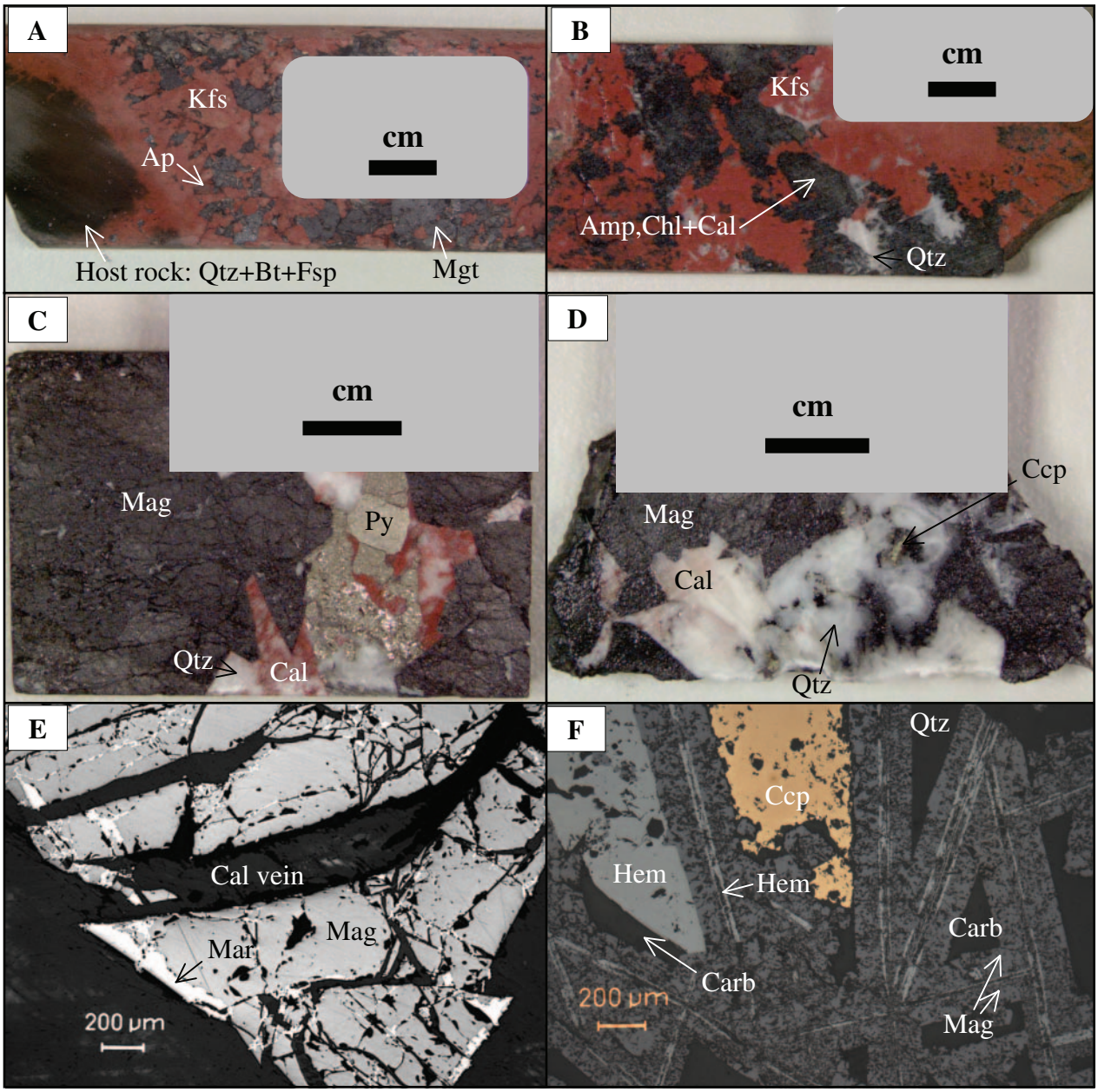

FIG. 5. Common alteration assemblages associated with IOCG prospects of the Olympic Dam district, represented in drill core samples and thin sections: magnetite-K-feldspar-calc-silicate assemblages (A-F), hematite-sericite-chlorite-carbonate assemblages (G-N). (A) and (B). Magnetite-K-feldspar-calc-silicate alteration, drill hole MRD1. (C) and (D). Magnetite-quartz-calcite-sulfide veins, drill hole MRD1. (E). Martite developing along margins and fractures of vein magnetite, drill hole MRD1. (F). Bladed magnetite developed after hematite, drill hole TI6. (G). Pyrite-chalcopyrite vein with specular hematite, drill hole TI6. (H). Vuggy hematitization zone, drill hole SAE6. (I). Early pyrite stringers cut by a quartz-chalcopyrite vein and hematite-chalcopyrite veinlets, drill hole SAE6. (J). Same sample as (I), showing detail of early fractured pyrite with hematite-chalcopyrite fracture infill. (K) and (L). Pyrite-chalcopyrite veinlets cutting magnetite. (M). Quartz-hematite-chlorite-sulfide–altered rock, drill hole TD2. (N). Replacement of magnetite and pyrite by chalcopyrite-hematite assemblage, drill hole TD2. Mineral abbreviations: Amp = amphibole; Ap = apatite; Bt = biotite; Cal = calcite; Carb = carbonate; Ccp = chalcopyrite; Chl = chlorite; Hem = hematite; Kfs = K-feldspar; Mag = magnetite; Mar = martite; Py = pyrite; Qtz = quartz.

or during magnetite-K-feldspar-calc-silicate alteration (Fig. 5F), although the occurrence of rare pyrrhotite inclusions in pyrite points to at least locally reducing conditions during formation of magnetite-bearing assemblages.

The central alteration zone in drill hole TI2 is occupied by multistage breccias, mafic dikes, and hematite-carbonate-chlorite alteration that cut and replace the magnetite-bearing assemblages. A narrower but similar zone is present in drill

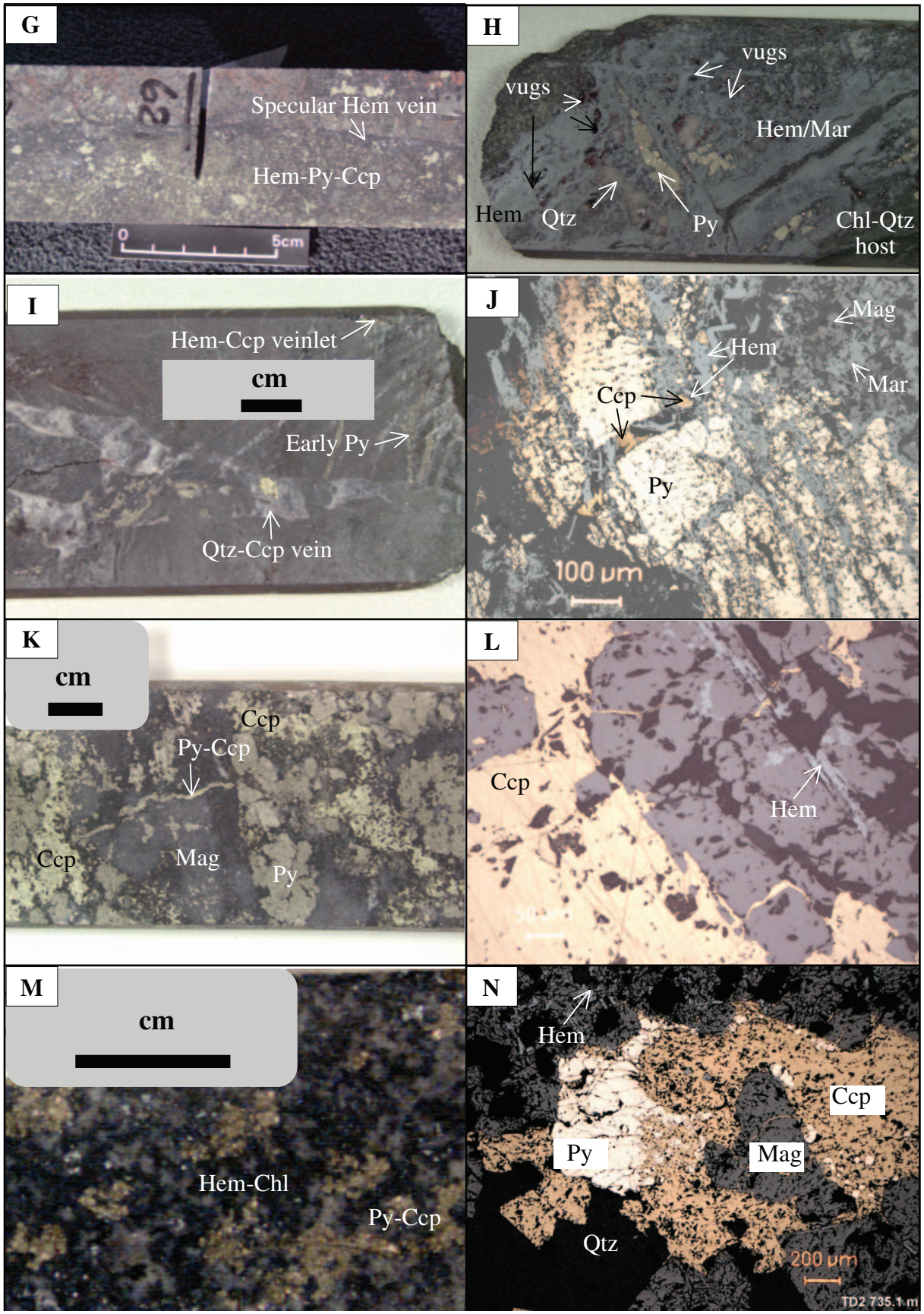
G
Specular Hem vein
Hem-Py-Ccp
0
5cm
H
vugs
vugs
Hem/Mar
Hem
Qtz
Py
Chl-Qtz host
I
Hem-Ccp veinlet
cm
Early Py
Qtz-Ccp vein
J
Mag
Hem
Mar
Ccp
Py
100 µm
K
cm
Ccp
Py-Ccp
Ccp
Mag
Py
L
Ccp
Hem
M
cm
Hem-Chl
Py-Ccp
N
Hem
Ccp
Py
Mag
Qtz
200 µm
TD2 735.1 m

FIG. 5. *(Cont.)*

hole BD1. Angular clasts of previously magnetite-altered meta-arkose and largely unaltered mafic dike rock occur in a matrix of comminuted wall rock, mafic silicate and/or mafic igneous rock, hematite-altered magnetite, carbonate, and chlorite. In contrast to the enclosing magnetite-K-feldspar-calc-silicate–dominated alteration zones, which typically contain 700 to 900 ppm Cu and 1.4 to 1.7 wt percent sulfur, this central zone of hematitic alteration contains only trace chalcopyrite and negligible pyrite (62 m at 200 ppm Cu, 700 ppm S: Tasman Resources, unpub. data). Microtextural evidence indicates that pyrite and chalcopyrite were replaced by hematite and carbonate in this central alteration zone. In comparison to other IOCG prospects in the Olympic Dam district, the low abundance of Cu associated with this central hematitic alteration zone at Titan is unusual and suggests hydrothermal leaching. The significance of this observation is considered below.

The intensity of martite replacement of magnetite decreases away from the central hematitic alteration zone, although minor late-stage hematite, carbonate, muscovite, and chlorite (replacement of amphiboles) persist throughout the magnetite-rich zones. Minor chalcopyrite is commonly present in the hematitic alteration, suggesting a second stage of copper deposition during hematitic alteration.

Emmie Bluff

As at the Olympic Dam and Prominent Hill deposits, the hematite-sericite-chlorite-carbonate assemblage is also well developed at the Emmie Bluff prospect (Gow et al., 1994). Two major zones of Fe oxide alteration about 3 km apart (Fig. 6) are characterized by coincident positive gravity and magnetic anomalies. The southern, discordant alteration zone contains veins and replacements within rhyodacite of the Gawler Range Volcanics; the veins contain skarnlike high-temperature mineral assemblages with combinations of clinopyroxene, actinolite, magnetite (<10 vol %), quartz, calcite, K-feldspar, pyrite, and allanite. Albite veins are found within the rhyodacite. Disseminated magnetite occurs in alteration selvages adjacent to the veins. Sulfides are low in abundance, with only very minor pyrite and traces of chalcopyrite.

The northern, strata-bound, alteration zone is up to ~150 m thick, ~3 km in diameter, and is hosted by chert, shale, and carbonate-bearing metasedimentary rocks of the upper Wallaroo Group as well as by brecciated zones of Donington Suite granite. Meta-arkosic rocks (quartz-K-feldspar-muscovite) underlying the upper Wallaroo Group are less altered, although rare magnetite and hematite veins are present. Alteration is crudely zoned downward from breccia and cataclasite zones, with intense hematite-chlorite-quartz alteration containing chalcopyrite-pyrite-bornite-covellite, to less brecciated magnetite-chlorite-pyrite–altered zones (Fig. 4C). The magnetite is interpreted to be a relic of earlier alteration, resembling magnetite-feldspar-calc-silicate alteration elsewhere in the district. The highest grade mineralized intersections contain up to 2.8 wt percent Cu and up to 0.6 ppm Au. Most chalcopyrite is intimately intergrown with pyrite and hematite that form part of the hematite-sericite-chlorite-carbonate assemblage. In detail, some chalcopyrite appears to have replaced pyrite. However, within the magnetite-bearing zone, chalcopyrite also occurs in contact with magnetite with no evidence for reaction, suggesting that some chalcopyrite may have initially precipitated as part of the early magnetite assemblage (Fig. 5K, L) or was deposited at the later hematitic stage but in equilibrium with magnetite.

Torrens

Magnetite-rich and hematitic alteration in the Torrens prospect area were intersected in drill hole TD2 (Figs. 2, 4). The intense metasomatism almost completely obliterated host-rock textures; rare relics of less altered host rock suggest that it was a fine-grained albitic metasedimentary rock, similar to the upper Wallaroo Group.

Magnetite-bearing alteration is characterized by pervasive and irregular replacement patches and veins of magnetite,

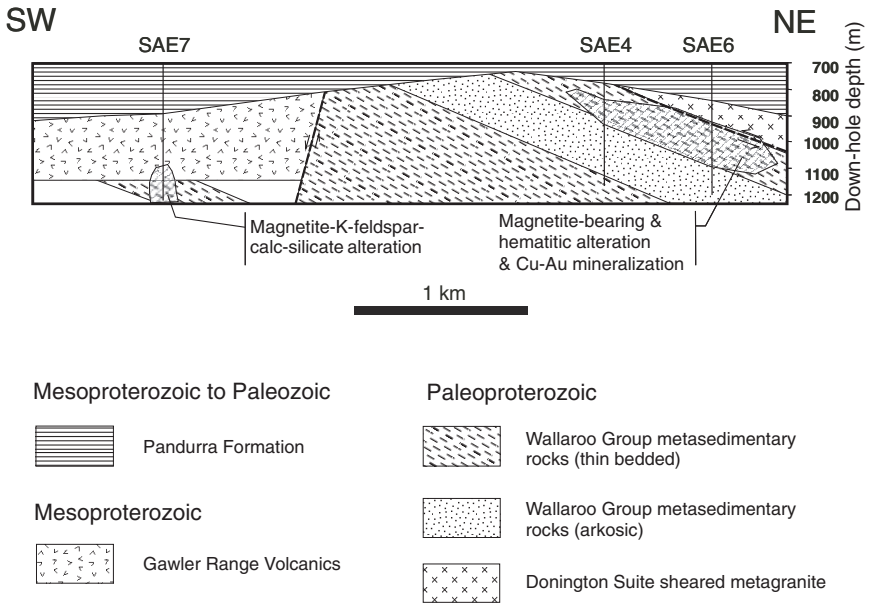

FIG. 6. Schematic cross section through the Emmie Bluff IOCG prospect. Modified after Gow (1996).

quartz, pyrite, K-feldspar, and apatite. Although no calc-silicate minerals are preserved, clinopyroxene and garnet are found as trapped phases within fluid inclusions in quartz. The relationships suggest the former presence of magnetite-K-feldspar-calc-silicate alteration at Torrens. Hydrothermal carbonate is locally abundant as "clasts" in pseudobreccia with magnetite-rich "matrix," suggesting that some carbonate may have formed in association with the magnetite-bearing alteration.

Hematitic alteration is well developed in several zones up to 30 m wide, overprinting the magnetite-bearing assemblages and, in places, associated with brecciation. Magnetite in these zones is extensively replaced by martite and fine-grained specular hematite with chlorite and white mica. Late-stage disseminated carbonate is also associated with chlorite and martite and/or hematite. Whereas chalcopyrite is intimately intergrown with pyrite that formed part of the magnetite-bearing assemblage, in detail some chalcopyrite appears to have replaced pyrite (Fig. 5N). We suggest that this chalcopyrite most likely formed during the hematitic alteration stage.

Analytical Methods

The nature of the fluids at several IOCG prospects in the Olympic Dam district was investigated by petrographic, microthermometric, and laser Raman microprobe methods at Geoscience Australia. Microthermometry was completed using a Linkam MDS 600 stage (–196° to +600°C), and Raman microanalysis was performed on a Dilor SuperLabram laser Raman microprobe.

A microanalytical study of selected fluid inclusions was completed at the CSIRO-GEMOC Nuclear Microprobe in Sydney. The nondestructive method of proton induced X-ray emission (PIXE) analysis of fluid inclusions is described by Ryan et al. (1993, 1995). Wherever possible, we selected shallow (<20 μm) fluid inclusions, >10 μm in diameter, to optimize analytical precision and accuracy.

Sulfur isotope compositions of sulfide minerals were determined at the University of Tasmania stable isotope laboratory. From the Olympic Dam district, 24 samples were analyzed using a Conventional technique (Robinson and Kusabe, 1975) with an overall precision of ±0.1 per mil. The samples for Conventional analysis were prepared by drilling sulfide minerals with a dental drill or by handpicking. To better understand the relationships between sulfur isotope composition and paragenetic position of the sulfides, 20 additional measurements were determined in situ on polished thin sections by the Laser ablation method (Huston et al., 1995), with an overall precision of ±0.3 per mil. For comparative purposes, seven additional samples of pyrite, chalcopyrite, and pyrrhotite were analyzed (three by Conventional technique, four by Laser ablation) from the Mount Woods inlier IOCG prospects (Fig. 3). Isotopic compositions of samples are reported in Table 1 and shown in Figure 10 relative to the CDT standard.

The oxygen and hydrogen isotope compositions of 20 samples of silicate minerals were determined at the Institute of Geological and Nuclear Sciences, New Zealand. Oxygen was extracted from silicates for isotope analyses using a CO_2 laser and BrF_5, similar to the method described by Sharp (1990). Values are reported in the familiar $\delta^{18}O$ notation relative to VSMOW (Table 2). Samples were normalized to the international quartz standard NBS-28, using a value of 9.6 per mil (‰). Values for four NBS-28 standards analyzed with the samples had values that varied by less than 0.1 per mil (K. Faure, pers. commun., 2004).

Hydrogen isotope (δD) values of the samples were determined using the method of Vennemann and O'Neil (1993). Samples were degassed at 200°C overnight to remove adsorbed water. Water was extracted from the hydrosilicates by heating to temperatures of about 1,300°C. All sample values are reported relative to VSMOW, and reproducibility of internal standards was better than ±3 per mil (Table 2). Sample values are normalized to the international biotite standard (NBS-30), assuming a value of –65 per mil.

Fluid Inclusions

Fluid inclusion types and microthermometry

The fluid inclusions from quartz and calcite in hydrothermal alteration and mineralization can be divided into three major types, based on phase relationships at room temperature and microthermometric behavior: (1) type A, vapor-rich, high-temperature inclusions; (2) type B, medium- to low-temperature, liquid-vapor inclusions; and (3) type C, high-temperature, halite-saturated hypersaline multiphase fluid inclusions (Fig. 7). In our study, type A and C inclusions were documented within magnetite-bearing assemblages at Titan (drill hole BD1), Torrens (drill hole TD2), and Emmie Bluff (drill hole SAE7). Some type A and type C inclusions survive in quartz grains in magnetite-bearing zones that were overprinted by hematitic assemblages (e.g., Torrens). Type B inclusions are ubiquitous in association with hematitic assemblages but also occur as trails of secondary inclusions in quartz of magnetite-bearing assemblages.

High-temperature brine inclusions have been previously reported only at Olympic Dam (Oreskes and Einaudi, 1992). Our work and that of Davidson et al. (2007) at Oak Dam demonstrates that the high-temperature hypersaline fluids were widespread throughout the Olympic Dam IOCG district, in association with magnetite-K-feldspar-calc-silicate alteration. An extensive dataset for the medium- to low-temperature type B liquid-vapor inclusions associated with hematitic alteration is available from the Mount Gunson area (Knutson et al., 1992), as well as for Olympic Dam (Oreskes and Einaudi, 1992) and Oak Dam (Davidson et al., 2007).

The gas phase in type A inclusions is dominated by water vapor with no detectable CO_2 or CH_4 (based on detection limits of about 0.1 mol % for CO_2 and 0.03 mol % for CH_4, using the laser Raman microprobe).

In addition to the ubiquitous halite crystals in type C hypersaline multiphase fluid inclusions, a number of other salt, silicate, and opaque daughter phases are present. Some of these minerals were identified using the Raman microprobe and include ferropyrosmalite ($(Fe,Mn)_8Si_6O_{15}(OH,Cl)_{10}$), white mica (Fig. 7C, D), magnetite, hematite, and chalcopyrite. In some cases, the multiphase brine inclusions contain minerals captured "accidentally" during inclusion growth (e.g., drill hole TD2, Fig. 7G, H). This is deduced from the relative size of the captured minerals and from inconsistency of their occurrence within the inclusion populations. Such

TABLE 1. Sulfur Isotope Values of Sulfides from the Olympic Dam District

Prospect	Drill hole	Depth (m)	Method	Spot	$\delta^{34}S_{sulfide}$ (‰) Py	Ccp	Po	Sph
			Mt Woods region					
Manxman	DD85 EN17		Laser ablation		–6.5	–6.3		
Manxman	DD89 EN61	322.10	Conventional		–2.0	–2.3		
Manxman	DD89 EN61	456.80	Conventional					
Manxman	DD89 EN61		Laser ablation	1	–3.6	–5.4	–6.4	
Manxman	EN33		Laser ablation	1			–0.4	
Peculiar Knob	PK1	326.90	Conventional				4.3	
			Olympic Dam region					
Titan	BD1	685.50	Conventional		–2.2	–3.2		
	BD1	685.50	Laser ablation	1	–4.0	–3.9		
	BD1	799.40	Conventional		–2.2	–2.8		
	BD1	799.40	Laser ablation	1	0.5	–2.5		
	BD1	801.80	Conventional		–2.9			
	BD1	868.00	Laser ablation	1	–1.1	0.2		
	BD1	868.00	Laser ablation	2	–4.1			
	BD1	897.40	Conventional		–2.1			
	BD1	917.00	Conventional		–3.1	–1.4		
Bill's Lookout	BLD1	581.30	Conventional		2.8			
	BLD1	730.70	Conventional		1.4			
	CSD1	960.00	Laser ablation	1	0.5	0.1		
	CSD1	960.00	Laser ablation	1	–1.2			
	CSD1	960.00	Laser ablation	2		1		
	CSD1	960.00	Laser ablation	3		1.5		
	DRD1	1,182.35	Conventional		–2.8			
Murdie Murdie	MRD1	859.30	Conventional		–1.2			
	MRD1		Conventional		–2.7			
Mount Gunson area	PY3	942.55	Conventional		2			
Emmie Bluff	SAE6	959.70	Laser ablation	1	5.4	5.2		
	SAE6	959.70	Laser ablation	2	3.1			
	SAE6	986.20	Laser ablation	1	10.3	12.1		
	SAE6	986.20	Laser ablation	2	9.6	9.4		
	SAE6	1,022.00	Laser ablation	1	6.3	8.3		
	SAE6	1,022.00	Laser ablation	2		7.9		
	SAE6	1,029.00	Conventional		7.6	8.5		
	SAE6	1,041.00	Laser ablation	1	2.6	12.5		
	SAR8	1,141.10	Conventional		3.1			
	SAR8	1,149.40	Conventional			3.3		
	SAR8	1,160.10	Conventional			2.8		
	SAR8	1,160.10	Laser ablation	1		3.1		6.4
	SAR8	1,160.10	Laser ablation	2				6.4
Torrens Dam	TD2	724.40	Conventional		0.3			
	TD2	724.40	Laser ablation	1	–0.1	0.5		
	TD2	724.40	Laser ablation	2		3.4		
	TD2	724.40	Laser ablation	3		3.8		
	TD2	735.10	Conventional			–0.1		
	TD2	746.60	Conventional		0.6			
	TD2	768.20	Conventional			0.4		
	TD2	806.10	Conventional		0.2			

Note: Mineral abbreviations: Ccp = chalcopyrite, Po = pyrrhotite, Py = pyrite, Sph = sphalerite

minerals detected in quartz from the hematitic alteration assemblage at Torrens included clinopyroxene and garnet (Figs. 5M, 7G, H) and can be interpreted as relics of the early magnetite-bearing assemblages that were overprinted by hematitic alteration. In microthermometric studies, complete homogenization was not attained in type C inclusions. They decrepitated at temperatures above ~400°C, and nonsalt daughter minerals did not dissolve fully prior to decrepitation.

The results of microthermometric measurements for the type B inclusions are shown in Figure 8. Our data indicate salinities from 1 to 6 wt percent NaCl equiv and homogenization temperatures from 150° to 300°C. Overall, including the available literature data (Knutson et al., 1992; Oreskes and Einaudi, 1992), there is a significant spread of the freezing point depression data for hematite-stage fluids, reflecting variable fluid salinities (up to NaCl saturation). Most type B fluid inclusions homogenized between 150° and 250°C.

Hypersaline liquid-vapor-multiple solid (L-V-nS) fluid inclusions are widely documented in IOCG systems of the Cloncurry district in association with regional albite-calc-silicate ±

TABLE 2. Oxygen and Hydrogen Isotope Compositions of Alteration Minerals from the Olympic Dam District

Prospect	Drill hole	Depth (m)	Rock	Mineral	$\delta^{18}O$	δD	T[1] (°C)	T[2] (°C	$\delta^{18}O_{water}$	δD_{water}
Emmie Bluff	SAE7	1,123.9	Magnetite alteration zone	Amp	7.7	–42		500	9.5	–21
Emmie Bluff	SAE7	1,168.0	Magnetite alteration zone	Amp	6.5	–40		500	8.3	–19
			Magnetite alteration zone	Amp	9.5			500	11.3	
			Magnetite alteration zone	Quartz	10.0			500	7.7	
Murdie Murdie	MRD1	821.7	Magnetite alteration zone	Amphibole	8.8	–36		500	10.6	–15
		834.3	Quartz-magnetite vein	Quartz	12.4		617	500	10.1	
				Magnetite	4.4			500	12.2	
		857.3	Quartz-magnetite vein	Quartz	13.0		595	500	10.7	
				Magnetite	4.6			500	12.4	
Titan	BD1	722.7	Quartz-magnetite vein	Quartz	10.9		773	500	8.6	
				Magnetite	5.0			500	12.8	
	TI006	620.9	Brecciation zone with iron-oxide-pyrite-chalcopyrite matrix (hematitic alteration)	Hematite	–0.9			250	8.6	
	TI006	622.9	Quartz-magnetite vein	Magnetite	4.7			500	12.5	
	TI006	732.2	Quartz-hematite-sulfide vein (hematitic alteration)	Hematite	0.3			250	9.8	
Torrens Dam	TD2	751.0	Hematitic alteration zone	Muscovite	7.7	–44		250	4.7	–9
	HUD1	481.2	Gawler Range Volcanics dacite	Biotite	5.3	–60		800	8.0	–39

[1] Calculated isotopic temperature based on the combination of $\beta^{18}O$ factors from Clayton and Kieffer (1991) for quartz and from Cole et al. (2004) for magnetite

[2] Temperature assumed for calculation of isotopic composition of water (see text)

magnetite alteration (e.g., Williams et al., 2001). Although K-feldspar is the dominant alkali feldspar in magnetite-bearing alteration assemblages in the Olympic Dam district, rather than albite, there appear to be similarities in fluid characteristics in the two IOCG districts. Especially striking is the similarity in the set of daughter minerals that persistently occur through the fluid inclusion mineral assemblages: halite, calcite, ferropyrosmalite, and magnetite. Interestingly, the hypersaline (L-V-nS) fluid inclusions in the Cloncurry district are associated with high-density vapor-rich CO_2 inclusions, whereas in our study vapor-rich type A inclusions lack CO_2.

Microanalytical (PIXE) results

The main aim of the PIXE study was to directly measure the copper contents of the fluids associated with IOCG systems in the Olympic Cu-Au province. A second goal was to characterize fluids in terms of the Br-Cl systematics to trace possible fluid sources. Selected results of PIXE analyses of fluid inclusion compositions are shown in Table 3 and Figure 9. Copper concentrations and Br/Cl ratios were successfully measured in the multiphase type C fluid inclusions associated with magnetite-bearing alteration (Table 3, Fig. 9A). Type B fluid inclusions associated with hematitic alteration did not yield quantitative data for copper, although the hematite-stage fluids were found to contain very low concentrations of copper compared to the magnetite-stage fluids (i.e., below the detection limits for the particular inclusions measured).

The fact that some of the magnetite-related fluids were extremely high in copper can be directly deduced from the observation that many of the multiphase fluid inclusions contain chalcopyrite crystals (confirmed by laser Raman microprobe). Thus, the extremely high measurements of the copper (2–4 wt %) for some inclusions are not surprising. The absence of chalcopyrite from other brine fluid inclusions from the same trails suggests that the observed chalcopyrite may have been trapped accidentally (cf. Fig. 7B). However, the measurements of copper concentrations of inclusions that lack visible chalcopyrite are still high (300–600 ppm copper) with potentially important implications for Cu-Au mineralization associated with magnetite-bearing alteration. Only minor copper was deposited in magnetite-rich assemblages, despite the brines carrying more than 300 to 600 ppm Cu. This suggests that saturation of copper minerals did not occur (e.g., the fluids were too hot, or redox conditions, pH, or sulfur concentrations were unfavorable), or the quantity of these fluids was not sufficient to produce appreciable copper mineralization at the magnetite alteration stage.

The Br/Cl ratios for magnetite-related fluids in the Olympic Dam district (Fig. 9B) lie beyond the range of typical magmatic and/or mantle values (Johnson et al., 2000; Kendrick et al., 2001), allowing for the possibility that the fluids originated as brines from a sedimentary basin or the crystalline basement.

Stable Isotopes

Sulfur isotopes

Within the Olympic Dam district our new data—together with those of Knutson et al. (1992) from the Mount Gunson area, Eldridge and Danti (1994) from Olympic Dam, and Davidson et al. (2007) from Oak Dam—indicate a significant range of sulfide $\delta^{34}S$ values from –14 to +12.5 per mil (Fig. 10). As a first approximation, these data imply two types of hydrothermal systems, the first characterized by negative to slightly positive $\delta^{34}S$ values (–14 to +4‰; Group I, Fig. 10) and the second characterized by a component

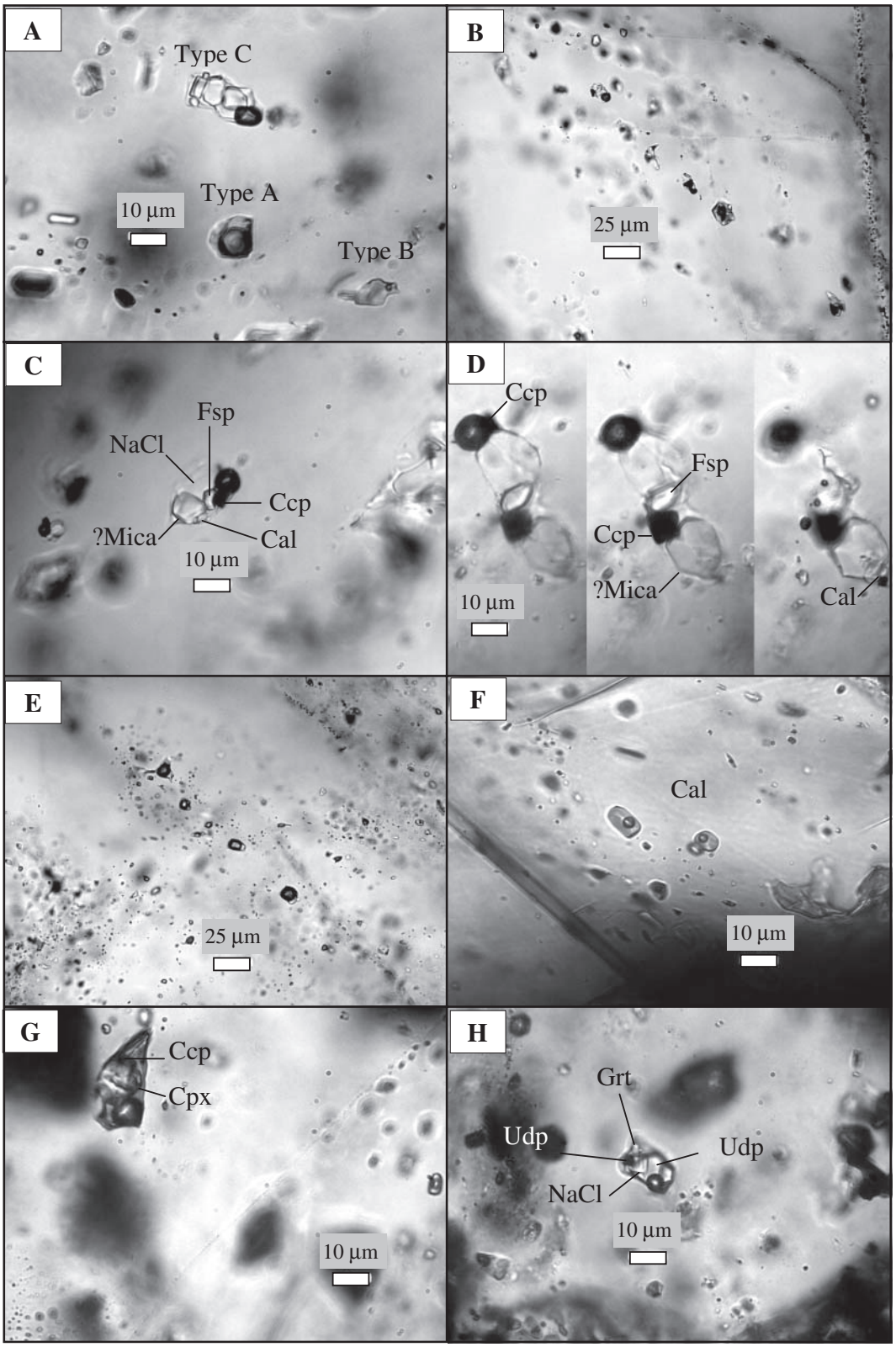

FIG. 7. Fluid inclusions of the IOCG prospects of the Olympic Dam district. (A). Three types of identified inclusions. (B)-(D). Type C inclusions (Titan prospect). (E). Type A inclusions filling a pseudosecondary fracture (Titan prospect). (F). Type B inclusions from calcite cutting fractured magnetite (Murdie Murdie prospect). (G) and (H). Multiphase fluid inclusions from Torrens prospect with relict minerals from magnetite-K-feldspar-calc-silicate alteration stage. Identified solid phases: Cal = calcite, Ccp = chalcopyrite, Cpx = clinopyroxene, Fsp = ferropyrosmalite, Grt = garnet, Udp = unidentified solid phases.

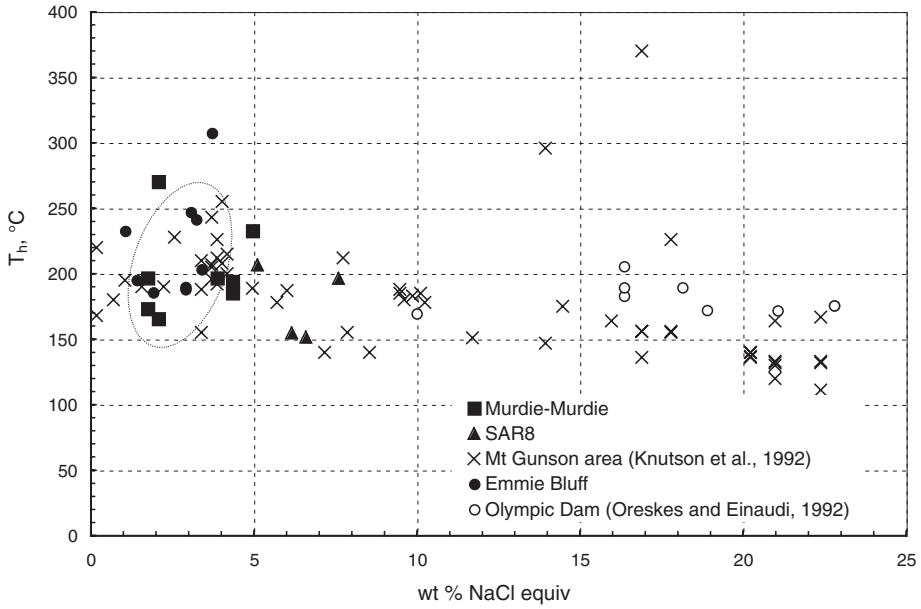

FIG. 8. Temperatures of final homogenization of B-type fluid inclusions vs. apparent salinities expressed in wt percent NaCl equiv.

with positive isotopic values from about 6 to 13 per mil (Group II, Fig. 10).

The widest range of sulfide $\delta^{34}S$ values within a single prospect was documented at Emmie Bluff (2.6–12.5‰; Fig. 10). The lowest value (2.6‰) corresponds to a generation of pyrite intergrown with magnetite and localized along compositional layering within the metasedimentary host rocks. This pyrite and magnetite predate the hematitic alteration assemblage because they are cut by chalcopyrite-hematite veins, and the magnetite is martitized (Fig. 5I, J). They may have formed as a part of the precursor magnetite-bearing assemblage, although most chalcopyrite and possibly minor pyrite grew during later hematitic alteration. The chalcopyrite values of 5.2 to 10.5 per mil are, overall, higher than the pyrite values of 3.1 to 10.3 per mil. Thus, the chalcopyrite is not in isotopic equilibrium with pyrite (cf. Ohmoto, 1972). Taking into account the textural evidence that the bulk of the chalcopyrite was deposited after pyrite, this indicates evolution of the bulk isotopic composition of sulfur in the fluids toward higher values. The highest $\delta^{34}S$ value (12.5‰) was measured in chalcopyrite from a specular hematite-chalcopyrite vein (Fig. 5J). This trend cannot be explained by simple redox reactions, as one would expect higher $\delta^{34}S$ values associated with the most reduced assemblages (i.e., chalcopyrite associated with magnetite) compared to the more oxidized hematite-bearing assemblages. Rather, the increase in the $\delta^{34}S$ values of chalcopyrite suggests that two different processes and/or sulfur sources could have contributed to the observed variation in the sulfur isotope composition at Emmie Bluff. These are considered further below.

Data for prospects in the Mount Woods inlier were obtained from Manxman and Cairn Hill prospects (Figs. 3, 10; drill holes DD89EN61, DD85EN17, and DD85EN33). The observed mineral assemblages are quite reduced, with pyrrhotite stable in drill holes DD89EN61 and DD89EN33, and the analyzed minerals, including pyrrhotite, are characterized by negative $\delta^{34}S$ values (from –6.5 to –0.38‰). As fractionation between aqueous H_2S and pyrrhotite is insignificant, these values indicate that $\delta^{34}S_{fluid}$ values were negative. Such values cannot be attributed to changing redox conditions and point to negative isotopic values of the sulfur source. Magmatic pyrrhotite from the Peculiar Knob gabbro (drill hole PK1) has a positive $\delta^{34}S$ value of 4.3 per mil (Fig. 10, Table 1), suggesting that some mafic magmas of Hiltaba Suite age in the Mount Woods inlier (Jagodzinski, 2005) could have assimilated crustal sulfur. By comparison, pyrite in the Bill's Lookout gabbro in the Olympic Dam district has somewhat lower $\delta^{34}S$ values of 1.3 and 2.8 per mil (Fig. 10, Table 1). In either case, sulfur sourced directly from such magmas or leached from the equivalent crystallized igneous rocks would also have a positive isotopic signature. If representative of the sulfur compositions in mafic magmas in this district, such sulfur would be an unlikely source of sulfur in the Manxman IOCG prospect.

Oxygen and hydrogen isotopes

We have attempted to constrain the formation temperatures of the magnetite-bearing alteration using quartz-magnetite geothermometry in samples from Murdie Murdie, where these minerals are intergrown (Table 2). The quartz-magnetite fractionation curve was based on the combination of $\beta^{18}O$ factors from Clayton and Kieffer (1991) for quartz and from Cole et al. (2004) for magnetite, as recently recommended by Cole et al. (2004). The three analyzed mineral pairs gave temperature estimates between 595° and 773°C. In the absence of the quantitative homogenization temperature data for fluid inclusions associated with magnetite formation in the studied prospects (see earlier), these temperatures cannot be independently verified. However, textural observations suggest that quartz postdates magnetite; thus, it is likely that

TABLE 3. Representative Results of PIXE Analyses of Elemental Abundances for Multiphase Brine Inclusions (Type C) from Quartz from K-feldspar–Calc-Silicate-Alkali Feldspar-Magnetite (CAM) Alteration Assemblages[1]

Prospect	Drill hole	Cl	K	Ca	Ti	Mn	Fe	Ni	Cu	Zn	As	Br	Rb	Sr	Ba	Au	Pb
Titan	BD1	122,429	69,247	40,015	1,500	6,532	277,179	<248	45,934	1,600	217	1,716	<2,421	3,349	3,950	<448	4,229
		<59,641	9,177	11,381	1,477	2,209	158,880	<244	19,826	706	<464	<3,276			2,163	<1,815	<1,760
		1,960	1,994	3,427	536	2,308	75,171	76	344	490	63	201	<549	792	719	<80	1,033
		15,314	16,397	3,360	306	2,395	86,863	<52	19,045	352	50	383	610	589	1,040	<100	2,223
Emmie Bluff	SAE7	335,110	37,395	38,414	<153	6,096	18,710	<152	499	2,031	2,182	910	<2,540	<2,481	7,092	<260	14,619
		207,346	23,104	96,396	<440	20,045	137,667	<460	679	4,623	1,378	1,330	<7,329	<7,309	5,624	<707	<5,564
		27,768	15,747	20,888	162	8,937	55,468	<125	288	1,379	285	655	<1,887	<1,878	1,705	<194	<616

Note: < = below the detection limit for a given fluid inclusion (cf. Ryan et al., 1995)
[1] All values in ppm

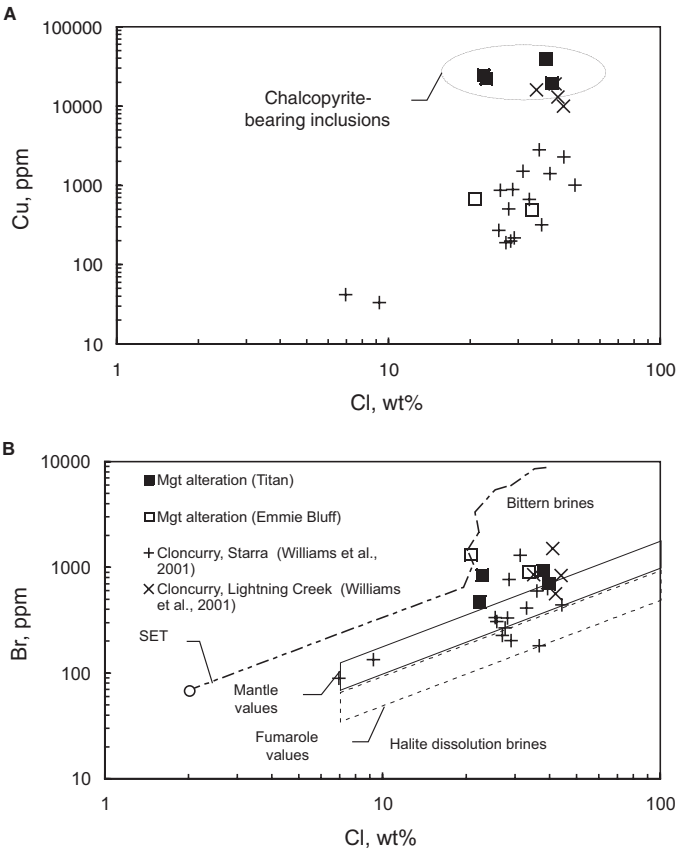

FIG. 9. Quantitative PIXE analyses of Br and Cl concentrations, and copper content of fluid inclusions associated with magnetite-K-feldspar-calc-silicate alteration. (A). Total measured copper content. (B). Br/Cl systematics of fluid inclusions. Reference mantle and fumarole fields are based on Johnson et al. (2000) and Bohlke and Irwin (1992), respectively. SET = seawater evaporation trend as summarized by Fontes and Matray (1993). Shown for comparison are data for the Cloncurry IOCG district of Queensland from Williams et al. (2001).

the calculated temperatures reflect isotopic disequilibrium and are unrealistically high. Postmagnetite deposition of quartz must have been from a fluid with $\delta^{18}O$ values somewhat lower than those of the fluid that precipitated magnetite.

Oreskes and Einaudi (1992) previously reported isotopic equilibrium temperatures for quartz-magnetite from Olympic Dam within the range ~420º to 540ºC. Thus, we used 500ºC for calculation of oxygen isotope composition of fluids in equilibrium with the analyzed magnetite-stage minerals (Table 2).

The limited data permit preliminary conclusions to be drawn on the origins of the water component of the fluids related to magnetite-bearing and hematitic alteration (Fig. 11). The composition of local magmatic water, based on a single analysis of fresh igneous biotite in the Gawler Range Volcanics, fits well within the generic box of magmatic water compositions associated with felsic magmas (Taylor and Sheppard, 1986). In contrast, compositions of fluids associated with the magnetite-bearing assemblage from Murdie Murdie and Emmie Bluff are consistent with fluids of metamorphic origin (Valley, 1986), which include fluids that have reacted

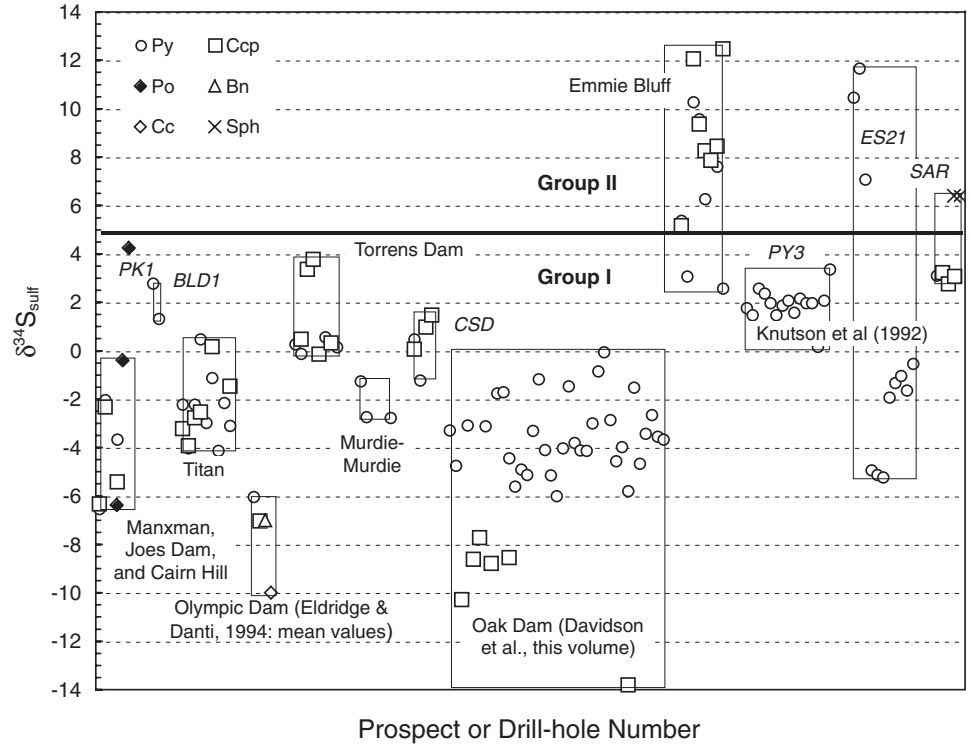

FIG. 10. Compilation of $\delta^{34}S$ data for sulfides from IOCG prospects of the Olympic Dam district. See Figures 1 to 3 for location of prospects. Data from Oak Dam (Davidson et al., 2007), regional alteration samples (Knutson et al., 1992, drill holes PY3 and EC21), and the median values for the Olympic Dam deposit (Eldridge and Danti, 1994) are included for comparison. Note that the horizontal axis does not have geologic meaning, but the locations are arranged from north (left) to south (right).

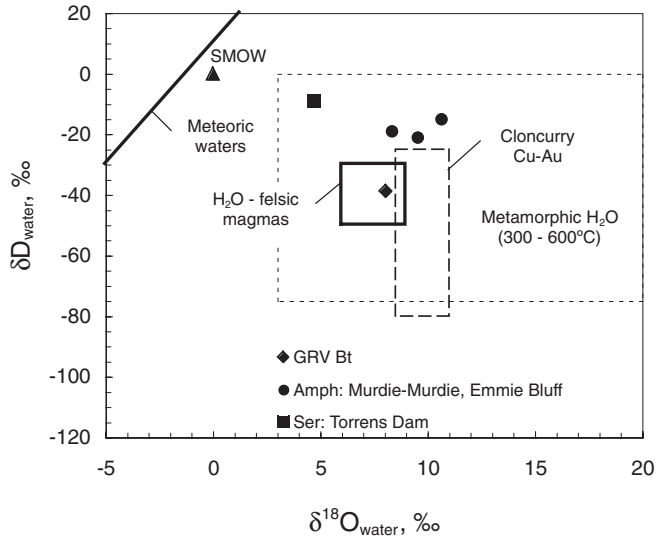

FIG. 11. $\delta^{18}O$ vs. δD systematics of IOCG-related fluids of the Olympic Dam district. Reference fields for magmatic and metamorphic waters are from Taylor (1986) and Sheppard (1986), respectively. Isotopic compositions of the fluids are calculated for the assumed temperatures of 800ºC (GRV Bt = magmatic biotite from the Gawler Range Volcanics), 500ºC (Amph = actinolite from magnetite-K-feldspar-calsilicate assemblages), and 250ºC (Ser = sericite from hematite-sericite-chlorite-carbonate assemblage). Range of data for the Cloncurry IOCG district of Queensland is based on Mark et al. (2004).

with metamorphic rocks at elevated temperatures. The single datum for the hematitic assemblage lies well outside the magmatic water box (Fig. 11).

Discussion

Two-stage evolution of subeconomic IOCG systems

The observed paragenetic relationships in subeconomic IOCG systems in the Olympic Dam district indicate a remarkably consistent pattern of hydrothermal evolution, with early magnetite-bearing alteration assemblages overprinted by hematitic assemblages. Our results support the two-stage model proposed by Gow (1996) for Emmie Bluff. In contrast, Haynes et al. (1995) argued that magnetite and hematite at Olympic Dam formed essentially coevally in different parts of the Olympic Dam Breccia Complex, during multiple overprinting hydrothermal cycles.

The general two-stage pattern of hematitic alteration overprinting magnetite-bearing assemblages is also observed in the other parts of the Olympic Cu-Au province at Moonta-Wallaroo and in the Mount Woods inlier (Skirrow et al., 2002). However, in addition to the magnetite-alkali feldspar-calc-silicate and hematitic alteration, deposits and prospects in these other two areas also involved magnetite-biotite alteration. The few cases where magnetite-biotite alteration has been observed together with magnetite-alkali feldspar-calc-silicate and hematitic alteration assemblages suggest that it

postdated the calc-silicate–bearing alteration and predated hematitic alteration (Conor, 1995; Hampton, 1997; Skirrow et al., 2002). The absence of magnetite-biotite alteration in the Olympic Dam district may reflect the relatively shallow crustal levels exposed in comparison with deeper levels in the other two areas (Skirrow et al., 2002, 2007). Currently available geochronology does not resolve the ages of magnetite-bearing and hematitic alteration in the Olympic Cu-Au province. The data are permissive of more than one cycle of magnetite to hematite alteration within the overall age brackets of 1595 to 1570 Ma (Skirrow et al., 2007).

Sources of fluids

The measured Br/Cl ratios of fluids related to magnetite-bearing alteration in the Olympic Dam district do not correspond to typical magmatic values, allowing for the possibility that the fluids originated as brines from a sedimentary basin or crystalline basement (Fig. 9A). The high salinities of the magnetite-related fluids could be explained either by their derivation from metasedimentary rocks of the Wallaroo Group, which contain scapolite or by liquid-gas phase separation of an initially supercritical fluid of moderate salinity (cf. Heinrich et al., 2004). Indeed, coexistence of type A and C inclusions in some samples (Fig. 7A) indicates that phase separation may have occurred.

Oxygen and hydrogen isotope compositions calculated for fluids related to magnetite-bearing and hematitic alteration are not consistent with a primary magmatic water source (Table 2, Fig. 11). Although the straightforward explanation is that these fluids are of metamorphic origin, they may also be products of local ^{18}O-enriched magmatic waters related to the Gawler Range Volcanics and Hiltaba Suite granites, reequilibration of primary magmatic waters with the host-rock sequences (i.e., metasedimentary rocks in the case of magnetite-related fluids, felsic igneous rocks in the case of hematite-related fluids), or mixing of the primary magmatic waters with fluids of nonmagmatic origin (i.e., metamorphic in the case of magnetite-related fluids, meteoric or seawater in the case of hematite-related fluids). Oreskes and Einaudi (1992) reported high $\delta^{18}O$ values for quartz from two samples of unaltered Hiltaba Suite granite from the vicinity of the Olympic Dam deposit (14.9 and 16‰) and suggested that these values characterize the granite, although whole-rock $\delta^{18}O$ values are quite typical of granitic rocks worldwide (9 and 9.1‰: Oreskes and Einaudi, 1992). It is not possible to deduce whether the high values are a result of subsolidus fluid-rock reequilibration. Taking into account that the Hiltaba Suite granite in this region can be classified as A-type (Creaser, 1989), high $\delta^{18}O$ values are unlikely to be primary, as these are typical for S-type magmas (Taylor and Sheppard, 1986).

Isotopic exchange with local felsic igneous rocks would have resulted in a substantial decrease of $\delta^{18}O$ values and an increase of δD values of the fluids (i.e., a trend toward the Torrens point in Fig. 11). Reaction with metamorphic rocks in the Olympic Dam district, which are likely to be enriched in ^{18}O, could account for the high $\delta^{18}O$ values calculated for magnetite-related fluids (Fig. 11).

Using the oxygen isotope composition of fresh igneous biotite from a Gawler Range Volcanics sample (5.3‰) and the plagioclase-biotite fractionation factor at near-magmatic temperatures (e.g., ~800°C), we can reconstruct the primary whole-rock isotopic composition (~6.8‰) of a hypothetical Gawler Range Volcanics dacite. As another constraint, we can use whole-rock values of ~9 per mil for the Hiltaba Suite granite host at Olympic Dam, published by Oreskes and Einaudi (1992). The compositional evolution of a fluid in equilibrium with each of these rocks at rock-dominated (R >> W, rock-buffered) conditions can be calculated simply as $\delta^{18}O_{fluid} = \delta^{18}O_{rock} - \Delta_{rock\text{-}fluid}(T)$ (Fig. 12; Campbell et al., 1984; Matveyeva et al., 1991).

The calculated fluid compositions based on literature values for magnetite-bearing assemblages from Emmie Bluff and Acropolis, and magnetite at Olympic Dam, are similar (Oreskes and Einaudi, 1992; Gow et al., 1994; Gow, 1996). The $\delta^{18}O$ values of some of the magnetite-bearing assemblages lie close to the values of the unbuffered "pristine" fluids of magmatic-like composition (Fig. 12). However, many compositions are significantly heavier. This is consistent with equilibration of a fluid with a country rock that is isotopically heavier than a hypothetical Gawler Range Volcanics dacite (i.e., >7‰). In contrast, values of $\delta^{18}O_{fluid}$ calculated for the hematitic alteration stage show a considerable range. At Emmie Bluff, Gow et al. (1994) and Gow (1996) used whole-rock and mineral isotope data to suggest a shift toward lower temperatures and lower $\delta^{18}O_{fluid}$ values due to the influx of evolved meteoric-hydrothermal waters. However, the data for minerals of the hematitic alteration stage (hematite and quartz) suggest isotopic temperatures that are too high (>390°C: Gow, 1996) when compared to our fluid inclusion data and temperatures of the hematite-related fluids elsewhere. We recalculated the mineral data of Gow (1996) using a temperature of 250°C (Fig. 12). As a result, the data split into two groups: high values associated with hematite and low values associated with quartz. The heavy oxygen in fluids in equilibrium with hematite is very similar to that associated with magnetite-related alteration, both at Emmie Bluff and elsewhere in the Olympic Dam district. We believe that this can result from hematite inheriting magnetite $\delta^{18}O$ values from the magnetite stage.

The single data point for hematite from the Torrens prospect also may reflect reequilibration with local volcanic rocks. Although no Gawler Range Volcanics are known from this area, Donington Suite granites are widespread. The relatively low $\delta^{18}O_{fluid}$ values are unlikely to have resulted from meteoric water influx, as the sulfur isotope compositions of sulfides are inconsistent with this hypothesis (see below).

Oxygen isotope compositions of fluids at Olympic Dam were calculated by Oreskes and Einaudi (1992), using the temperatures determined from magnetite-quartz and hematite-quartz pairs and assuming isotopic equilibrium between iron oxide minerals and quartz. The lower end of their isotopic temperature range (200°–360°C) is consistent with their fluid inclusion data (mean homogenization temperature ~200°C, see Fig. 8), and they favored input of meteoric waters to explain the relatively low $\delta^{18}O_{fluid}$ values associated with hematite. Figure 12 shows that the Olympic Dam data are also consistent with a scenario of buffering of the fluids by the Hiltaba Suite granite host rock.

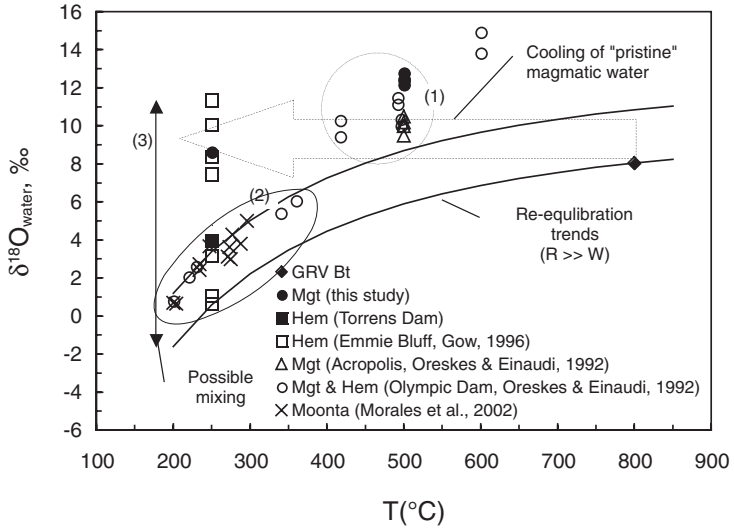

FIG. 12. Calculated $\delta^{18}O$ composition of the IOCG-related fluids as a function of temperature. The solid lines track hypothetical changes in isotopic composition of fluids in equilibrium with the Gawler Range Volcanics and Hiltaba Suite granites at rock-buffered conditions. Numbers adjacent to the outlined fields identify possible scenarios controlling oxygen isotope composition of hydrothermal fluids. See text for discussion. Abbreviations: GRV Bt = magmatic biotite from the Gawler Range Volcanics, Mgt = magnetite from magnetite-K-feldspar-calc-silicate assemblages, Hem = hematite from hematite-sericite-chlorite-carbonate assemblages. Data for Acropolis and Olympic Dam (Oreskes and Einaudi, 1992) are for Fe oxide and silicate minerals of the magnetite and hematite alteration.

Morales et al. (2002) presented oxygen isotope analyses from quartz veins and chlorite from the Moonta Cu-Au deposits in the southern Olympic Cu-Au province. The results are plotted in Figure 12 based on the mean fluid inclusion homogenization temperatures reported by these authors. These data are also consistent with the trend constructed for reequilibration with the Gawler Range Volcanics and Hiltaba Suite granites.

Sources of sulfur

The Olympic Dam district contains Fe-Cu sulfides associated with magnetite and hematite with a wide range of $\delta^{34}S$ values, from –14 to +12.5 per mil (Fig. 10). The large negative values in this range are associated with hematitic alteration in the Olympic Dam deposit (Eldridge and Danti, 1994) and in the Oak Dam prospect (Davidson et al., 2007). Most $\delta^{34}S$ values from other IOCG systems in the Olympic Dam district, whether for sulfides associated with magnetite-bearing or hematitic assemblages, lie in the range of –4 to +4 per mil. In the Mount Woods inlier, pyrrhotite, pyrite, and chalcopyrite in magnetite-bearing assemblages of the IOCG prospects have $\delta^{34}S$ values ranging from –6.5 to –0.4 per mil. Sulfur in this system was unlikely to have been sourced from local mafic rocks (e.g., the Peculiar Knob gabbro, if its pyrrhotite value of +6.4‰ is representative). The available data suggest that a metasedimentary rock source of sulfur is more likely. Except for the Titan prospect, IOCG alteration and mineralization assemblages in the Olympic Dam district are more oxidized and lack pyrrhotite. Pyrite and chalcopyrite that formed as part of magnetite-bearing assemblages, for example at Titan, Murdie Murdie, and in drill holes CSD1 and DRD1, have $\delta^{34}S$ values of –4.1 to +1.5 per mil (Table 1). Given the likely formation temperatures of 400° to 500°C and moderately reduced conditions of magnetite-pyrite-chalcopyrite deposition where we would expect relatively low $[HSO_4^- + SO_4^{2-}]/[H_2S + HS^-]$ ratios, these sulfide $\delta^{34}S$ values are consistent with a $\Sigma\delta^{34}S_{fluid}$ value of around 2 per mil (Fig. 13A). Although nonunique (see below), possible sources of this sulfur include magmatic-hydrothermal fluids or sulfur leached from igneous rocks (Ohmoto, 1986). Sulfides in magnetite-bearing assemblages at the Emmie Bluff prospect have quite different sulfur isotope compositions. Paragenetically early pyrite, some of which is associated with magnetite, has $\delta^{34}S$ values from 2.6 to as high as 10.3 per mil (Table 1). Chalcopyrite, which commonly replaced pyrite and formed predominantly during the hematitic alteration and Cu-Au mineralization event, has either similar or higher $\delta^{34}S$ values than the pyrite. A possible explanation of these characteristics is presented in Figure 13B. Early pyrite associated with magnetite may have formed from fluids similar to those associated with magnetite-bearing assemblages in other IOCG prospects (~2‰) but was modified during the hematitic alteration event, when a different, isotopically heavy fluid was involved. At the relatively oxidized conditions of hematitic alteration and mineralization, the chalcopyrite $\delta^{34}S$ values of up to 12.5 per mil at Emmie Bluff are consistent with a $\Sigma\delta^{34}S_{fluid}$ value ~20 per mil. This requires either an oxidized metasedimentary rock source or seawater or evaporitic water source of sulfur.

Figure 13B shows that the $\delta^{34}S$ values of pyrite and chalcopyrite associated with magnetite could theoretically result from deposition from a highly oxidized fluid with a $\delta^{34}S_{\Sigma S}$ value of around 20 per mil. However, we consider this very unlikely because the magnetite-bearing assemblages consistently point to relatively reduced conditions. In contrast, Eldridge and Dante (1994) reported consistently negative

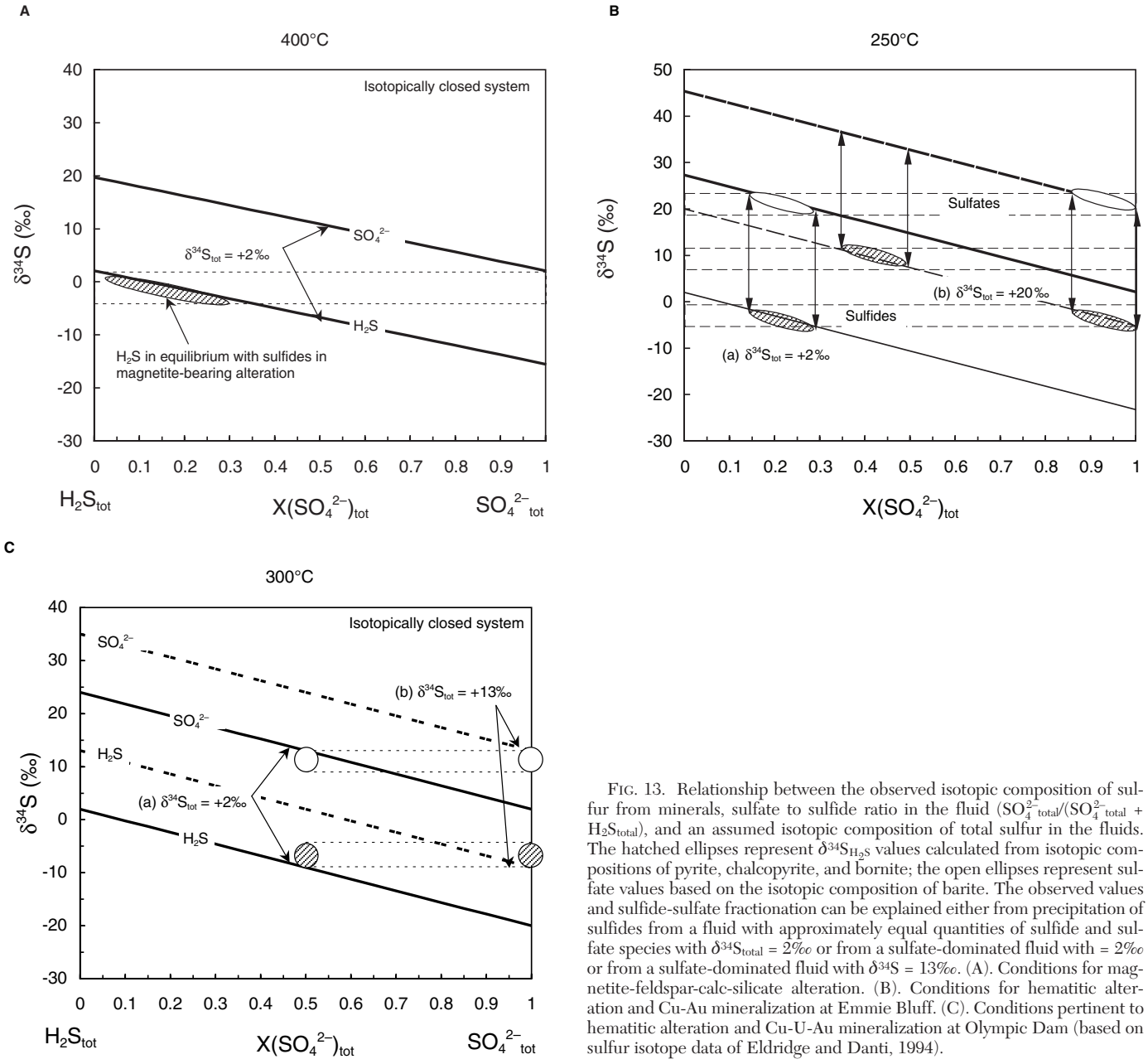

FIG. 13. Relationship between the observed isotopic composition of sulfur from minerals, sulfate to sulfide ratio in the fluid ($SO_4^{2-}{}_{total}/(SO_4^{2-}{}_{total} + H_2S_{total})$, and an assumed isotopic composition of total sulfur in the fluids. The hatched ellipses represent $\delta^{34}S_{H_2S}$ values calculated from isotopic compositions of pyrite, chalcopyrite, and bornite; the open ellipses represent sulfate values based on the isotopic composition of barite. The observed values and sulfide-sulfate fractionation can be explained either from precipitation of sulfides from a fluid with approximately equal quantities of sulfide and sulfate species with $\delta^{34}S_{total}$ = 2‰ or from a sulfate-dominated fluid with = 2‰ or from a sulfate-dominated fluid with $\delta^{34}S$ = 13‰. (A). Conditions for magnetite-feldspar-calc-silicate alteration. (B). Conditions for hematitic alteration and Cu-Au mineralization at Emmie Bluff. (C). Conditions pertinent to hematitic alteration and Cu-U-Au mineralization at Olympic Dam (based on sulfur isotope data of Eldridge and Danti, 1994).

isotopic values for sulfides from Olympic Dam (mean values from $\delta^{34}S_{pyrite}$ = –5.2‰ to $\delta^{34}S_{chalcocite}$ = –10‰, standard deviation of 2‰; Fig. 10) and a mean value for barite of 11 per mil consistent with deposition from a fluid with a $\Sigma\delta^{34}S$ value of around 2 per mil, if fluid [HSO_4^- + SO_4^{2-}] contents approximately equalled [H_2S + HS^-] contents (Fig. 13C). This is reasonable for chalcopyrite-pyrite-hematite assemblages, particularly where early magnetite was replaced by hematite sulfides (Oreskes and Einaudi, 1990; Reeve et al., 1990; Haynes et al., 1995). Alternatively, barite, chalcocite, and perhaps some bornite at Olympic Dam were precipitated from an SO_4^{2-}-dominant fluid with bulk $\delta^{34}S$ = 13 per mil (Fig. 13C).

Further evidence for a ^{34}S-enriched sulfur source in the Olympic Dam district is provided by the data of Knutson et al. (1992) for the Mount Gunson area. The studied drill holes, EC21 and PY3 (Fig. 2), intersect strongly altered Gawler Range Volcanics. Although most of the contained pyrite has $\delta^{34}S$ values of –5.2 to +2.6 per mil, a few samples had distinctly different $\delta^{34}S$ values from 7.1 to 11.7 per mil (Fig. 10). Knutson et al. (1992) interpreted these positive values in terms of fluid interaction with an oxidized host rock and precipitation of sulfate minerals that were later remobilized and locally reduced. We believe that these data can be equally well explained by a sedimentary rock surce of heavy sulfur.

In the Moonta-Wallaroo district, $\delta^{34}S$ data for sulfides in Wallaroo Group metasedimentary and metavolcanic rocks (–1.5 to +4.6‰) and Cu-Au vein deposits (–2.3 to +6.4‰) are similar (Morales et al., 2002). If the values for metasedimentary

rock-hosted sulfides are representative of the Wallaroo Group elsewhere, it cannot account for the strongly positive $\delta^{34}S$ values associated with hematitic alteration and Cu-Fe sulfide mineralization at Emmie Bluff, Mount Gunson area, or Olympic Dam. Other potential ^{34}S-enriched sulfur sources are scapolite in the Wallaroo Group, Proterozoic seawater, or sulfate-rich evaporitic waters.

In summary, sulfur in fluids associated with magnetite-pyrite-chalcopyrite–bearing assemblages was sourced dominantly from magmas or leached from igneous rocks in the Olympic Dam district, whereas in the Mount Woods inlier metasedimentary rock sources (biogenic sulfur) were involved in some IOCG systems. Sulfur in hematitic alteration and mineralization assemblages had diverse origins and probably included strongly ^{34}S-enriched metasedimentary rock sources and/or the Proterozoic hydrosphere.

Thermodynamic modeling of Cu-Au transport and deposition

Several geologic and chemical models of ore formation have been published for the Olympic Dam IOCG deposit (Oreskes and Einaudi, 1990, 1992; Reeve et al., 1990; Haynes et al., 1995), whereas models for subeconomic mineralization in the Olympic Dam district have been presented only for the Emmie Bluff prospect (Gow et al., 1994; Gow, 1996). The common theme of most models is the interplay between relatively reduced, magnetite-stable, high-temperature fluid and oxidized, hematite-stable, lower temperature fluid (Table 4). Key differences between models relate to the role of granites versus other sources of metals and fluids, the timing of fluid-rock interaction, and which of the two fluids carried the ore metals. The viability of fluid mixing as an ore-forming process at Olympic Dam was demonstrated by Haynes et al. (1995). Although new thermodynamic data for Fe, Cu, and Au have become available since 1995, they do not dramatically change the conclusions of that paper. A two-stage water-rock interaction hypothesis, advocated by Gow et al. (1994) and Gow (1996) for Emmie Bluff has not been modeled thermodynamically. Our geologic and mineralogical studies of other subeconomic prospects in the district suggest that a two-stage model of water-rock interaction may be widely applicable to the formation of IOCG systems. In the following, we use thermodynamic modeling to evaluate whether two-stage water-rock interaction can account for the observed mineral assemblages and Cu-Au grades in subeconomic IOCG systems of the Olympic Cu-Au province.

In this paper, we consider the interaction of a preexisting magnetite-bearing assemblage, formed at high temperature and from high-salinty fluids, with lower temperature and less saline oxidized fluids, using the HCh package for geochemical modeling (Shvarov and Bastrakov, 1999; Shvarov et al., 1999). Thermodynamic properties of the model species were taken from a Geoscience Australia version of the UNITHERM database (Shvarov and Bastrakov, 1999; Shvarov et al., 1999) consistent with the web-enabled FreeGs database (Bastrakov et al., 2004). The modeling was completed at 250°C and saturation pressures of pure water. The salinity of the fluid prior to water-rock equilibration was set to 3 *m* NaCl; other fluid compositional parameters were constrained by rock-buffered granite-rock equilibrium (at a water/rock wt ratio of ~0.03) in a closed-box system open to oxygen (a sliding f_{O_2} scale). We have considered a simplified chemical system of H-O-Cl-S-Na-K-Mg-Fe-Si-Al-Cu-Au, which would be a reasonable approximation for a felsic rock type, with the preequilibration composition of granite specified as a mixture of quartz, K-feldspar, albite, muscovite, phlogopite, annite, magnetite, and pyrite ± chalcopyrite. Starting compositions for the modeling are provided in Appendix 2.

Reduction of the oxidized fluid by interaction with magnetite-bearing alteration: In this model (Table 4), a magnetite-rich body acts as a chemical trap for copper and gold transported in an oxidized, sulfate-dominated fluid. Precipitation of ore components results from the reduction of sulfate due to magnetite oxidation (Fig. 14A). As a first approximation, the impact on copper solubility is modeled for a system that is closed with respect to all components except f_{O_2}. Figure 14A shows the change in the ore assemblage and copper solubility in response to the change of redox conditions. A dramatic drop in the solubility of copper (~2 orders of magnitude) occurs at the chalcocite-bornite reaction boundary, followed by a minor drop toward the hematite-magnetite transition and then toward the pyrrhotite stability field. Thus, simple reduction of an oxidized fluid similar to that associated with hematitic alteration can be an effective driving force for precipitation of copper, if that fluid carried copper.

TABLE 4. Possible Geochemical Models for IOCG Mineralization in the Olympic Dam District

Model group	Mechanism	Ore fluid	Precipitating agent/substrate	Reference
Fluid mixing		Oxidized Cu-Au-U–bearing fluid	Reduced fluid without ore metals	Haynes et al. (1995)
Fluid mixing		Reduced Cu-Au–bearing fluid	Oxidized U-bearing fluid	Reeve et al. (1990)
Fluid-rock interaction	Simple fluid reduction	Oxidized Cu-Au-U–bearing fluid	Reduced barren magnetite-rich assemblage	Haynes et al. (1995)
Fluid-rock interaction	Upgrading of preexisting mineralization	Oxidized fluid without ore metals	Reduced magnetite-rich assemblage with subeconomic Cu-Au mineralization	This study; after Oreskes and Einaudi (1990, 1992) and Gow (1996)

Note: Models of Haynes et al. (1995), Reeve et al. (1990), Oreskes and Einaudi (1990, 1992) were specifically developed for the Olympic Dam deposit, whereas that of Gow (1996) was for the Emmie Bluff prospect; these models do not necessarily apply to other IOCG mineralization in the district (see text)

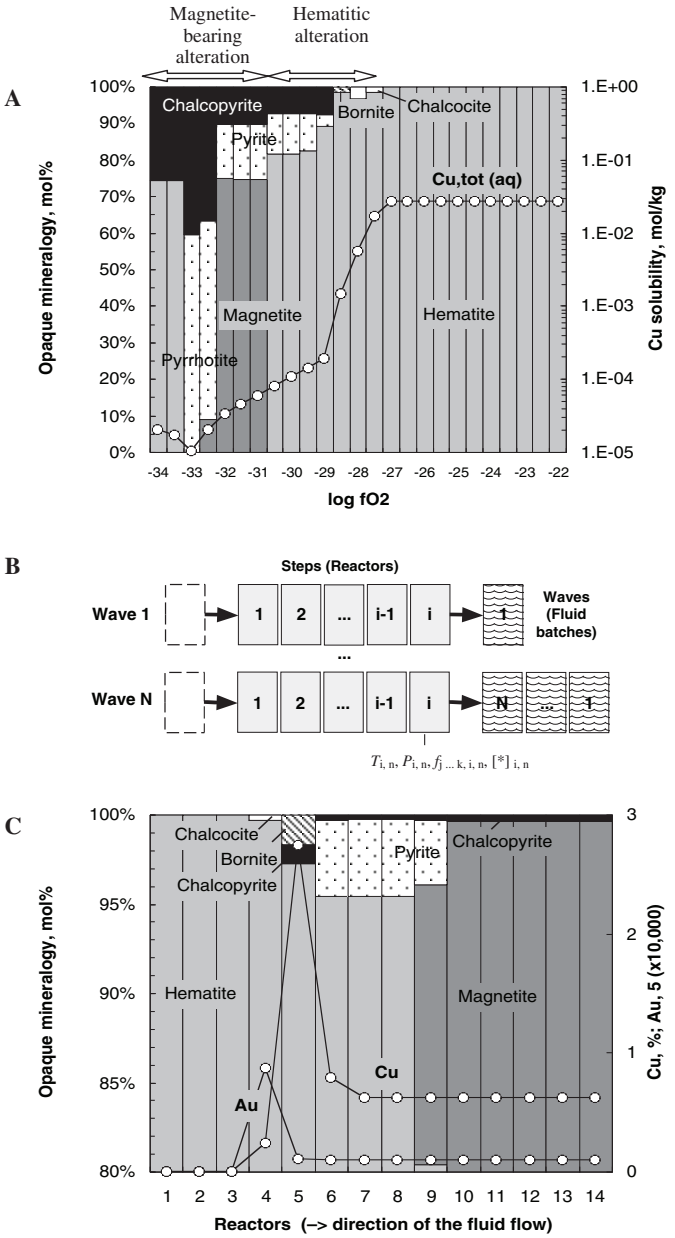

FIG. 14. Water-rock interaction models for Cu and Au precipitation in IOCG systems. (A). Copper precipitation by reduction of a copper-gold–bearing oxidized (hematite-stable) fluid interacting with a magnetite-bearing assemblage. (B). Cartoon showing the calculation principle of progressive fluid-rock interaction along a one-dimensional fluid-flow path following the "step-flow-through reactor" modeling technique. Each reactor is characterized by its own temperature (T_i), pressure (P_i), chemical potentials of perfectly mobile components (f_i, if any), and bulk chemical composition ([*]). Equilibrium compositions of consecutive reactors are calculated through a number of passes (waves) of fluid batches through the system. (C). Copper and gold precipitation by progressive oxidation and upgrading of preexisting copper-gold mineralization. The figure is a snapshot of the mineral zoning developing in response to the infiltration of the oxidized fluid. Note the enrichment fronts of copper minerals and the predicted sequence of the copper minerals. An intrinsic water-to-rock ratio is set to 10. The fluid infiltration front is at reactor 9.

Upgrading of preexisting Cu-Au mineralization: Dissolution of preexisting Cu-Au mineralization and reprecipitation at higher grades (upgrading) also has been examined. The oxidized H_2O-NaCl fluid is chemically equilibrated with an oxidized Gawler Range Volcanics felsic rock lacking Cu and Au; the initial composition of the fluid was calculated as discussed above, with the f_{O_2} value set ~8 log units above the hematite-magnetite buffer ($\log f_{O_2} = -27$, in the chalcocite stability field, compared to –34.9 for the hematite-magnetite buffer at 250°C). This fluid, lacking Cu and Au, is isolated from its source and progressively reacted with magnetite using the step-flow-through reactor numerical technique (Fig. 14B; cf. Heinrich et al., 1996). In this model, it is assumed that the magnetite-rich body acted as a source of Cu and Au (0.5 wt % Cu, 0.5 ppm Au), which were progressively upgraded by a dissolution-reprecipitation mechanism. This model offers a plausible explanation for the apparent lack of measurable amounts of copper in the fluids related to hematitic alteration examined in this study. The infiltration of the oxidized fluids into a magnetite domain oxidizes magnetite and leaches ore minerals and sulfur; the fluid reduction along the infiltration path results in the zoned reprecipitation of sulfides in the sequence: chalcocite, bornite + chalcopyrite, and chalcopyrite + pyrite (Fig. 14C). The model results in grades of up to 3 wt percent Cu and 5 ppm Au, similar to those observed in narrow intervals in the studied subeconomic IOCG systems. However, the total mass of ore metals accumulated in the model will be limited by the initial amount of copper and gold introduced during the early magnetite-forming event.

The upgrading mechanism can account for the paragenetic and mineralogical observations at most of the subeconomic IOCG systems in the Olympic Dam district, including Titan, Torrens, and Emmie Bluff. The simple reduction mechanism in which additional copper is introduced at the hematitic alteration stage may have been important for the formation of major IOCG deposits.

Summary and Conclusions

This study of fluid evolution in subeconomic Fe oxide Cu-Au systems of the Olympic Dam district indicates a diversity of possible origins for these deposits. The available geologic data suggest two broad stages of hydrothermal activity. Weakly Cu-Au mineralized bodies of magnetite-bearing alteration were present prior to formation of subeconomic as well as some major Cu-Au bodies in the Olympic Cu-Au province (Magnetite stage, Fig. 15). Our study has shown that the fluids associated with relatively reduced, high-temperature (~450°–500°C) magnetite-bearing alteration were Cu-rich hypersaline brines, yet they failed to produce extensive high-grade Cu mineralization. The Br/Cl ratios, and S, O, and H isotope compositions of the magnetite-related fluids indicate magmatic or leached igneous rock sources of sulfur but also suggest extensive exchange reactions with metasedimentary rock sequences in the fluid source and/or pathway regions.

The new stable isotope, fluid inclusion, and geochemical data indicate that the hematite-forming fluids experienced varying amounts of chemical exchange with host rocks in the Olympic Dam district, resulting in diverse sulfur and oxygen isotope signatures of the oxidized fluids (Hematite stage, Fig. 15). The oxidized fluids associated with Cu-U-Au mineralization and hematization at the Olympic Dam deposit appear to have reequilibrated more extensively with igneous rocks (mafic

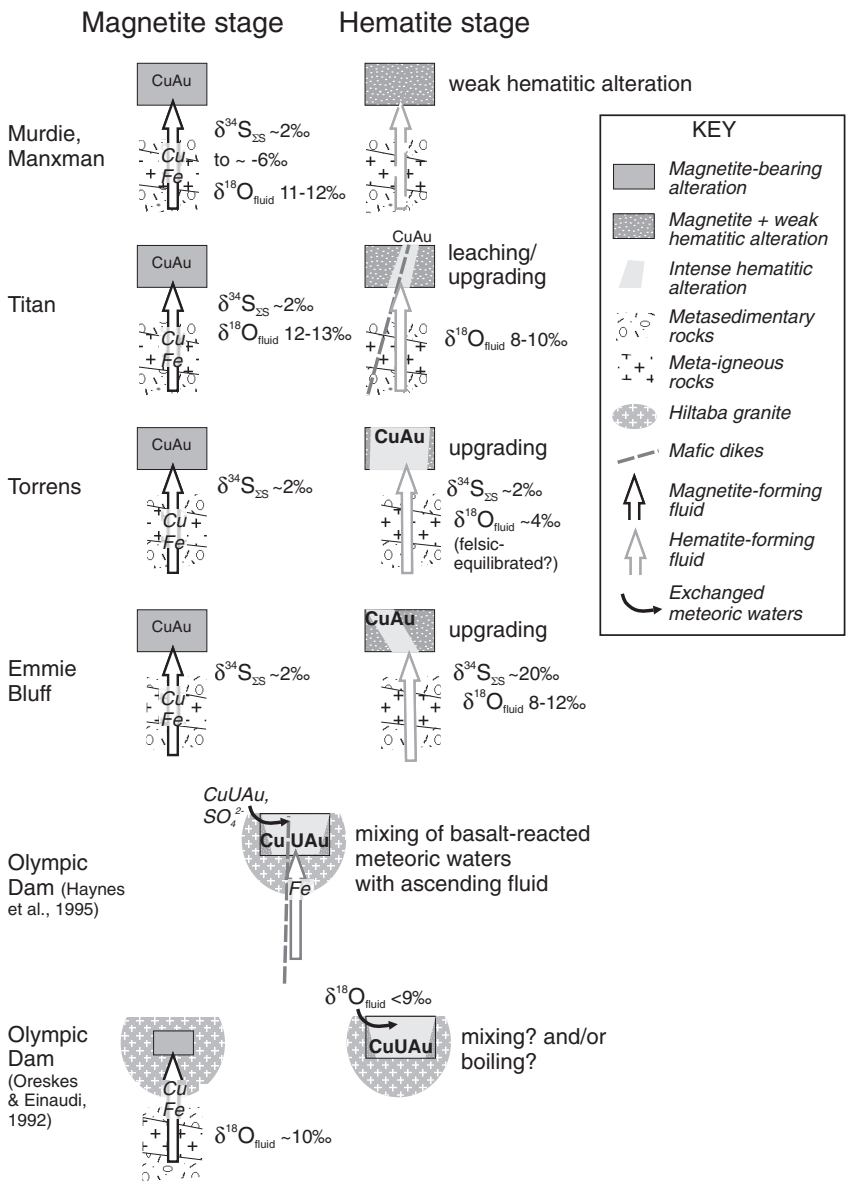

FIG. 15. Schematic summary of two-stage chemical and isotopic evolution in subeconomic prospects of the Olympic Dam district (Murdie, Manxman, Titan, Torrens, Emmie Bluff), in comparison with the Olympic Dam deposit. The two scenarios illustrated for Olympic Dam are based on the models of Haynes et al. (1995) and Oreskes and Einaudi (1992; see text). A third model (not shown) involves Cu transport by a deeply sourced ascending oxidized fluid, either mixing with or postdating magnetite-forming fluids (Johnson and McCulloch, 1995). The sulfur and oxygen isotope compositions of sulfide and silicate minerals in magnetite-bearing alteration in subeconomic prospects are generally consistent with fluid $\delta^{34}S_{\Sigma S}$ compositions of ~2 per mil and $\delta^{18}O$ compositions of ~11 to 13 per mil. At the hematitic alteration stage, isotopic compositions, fluid and sulfur sources, and alteration-mineralizing processes were more variable. They included hydrothermal leaching of magnetite-stage sulfide mineralization (e.g., Titan) and hydrothermal upgrading of such earlier formed Cu-Au mineralization (e.g., Torrens, Emmie Bluff). Olympic Dam may differ chemically from subeconomic prospects as a result of the combination of different sources of ore metals and sulfur, higher oxidation state during mineralization, and depositional mechanisms (e.g., fluid mixing; see text and Skirrow et al., 2007).

and felsic) than in the subeconomic IOCG systems, at temperatures as low as ~150°C (Oreskes and Einaudi, 1992; Haynes et al., 1995; Johnson and McCulloch, 1995). This comparison suggests that the process of relatively low temperature fluid-rock reaction was crucial for generation of Cu-U-Au–rich oxidized ore fluids. Previous chemical modeling has shown that reduction of Cu-Au–rich oxidized fluids is a viable mechanism of formation of major hematite-dominated IOCG deposits. In contrast, our observations of the weakly mineralized IOCG systems are consistent with a process of upgrading of preexisting low-grade Cu-Au mineralization in magnetite-bearing alteration zones by Cu-Au–poor oxidized brines.

Sulfur isotope data for sulfides at Olympic Dam are consistent with late-stage influx of highly oxidized (surficial?) waters

carrying highly ^{34}S-enriched sulfate, recorded in hypogene chalcocite mineralization. This is not observed in the subeconomic deposits. The major sources of copper and other metals in the Olympic Dam deposit were at least partly external to the host Roxby Downs granite and involved mantle-derived rocks or magmas (Haynes et al., 1995; Johnson and McCulloch, 1995). In contrast, new data for subeconomic prospects in the Olympic Dam district presented in this study and by Skirrow et al. (2007) indicate recycling of metals and sulfur from the local host rocks, with limited or no input from mantle-derived sources.

Acknowledgments

The authors wish to thank our colleagues in Geoscience Australia—Patrick Lyons, Nick Williams, Peter Milligan, Geoff Fraser, Peter Southgate, and Chris Pigram—for their support and valuable discussions on many and varied aspects of this work. The study was conducted under the auspices of the National Geoscience Agreement, as part of the Gawler Project in collaboration with the Department of Primary Industries and Resources South Australia. We thank Michael Schwarz, Paul Heithersay, Sue Daly, and Brian Logan for their ongoing support in this collaboration. Andy Barnicoat and Jon Clarke reviewed an earlier version of the manuscript and suggested significant improvements. Thorough reviews by Geordie Mark and James Cleverley improved the manuscript, for which we are thankful. Editorial handling by Garry Davidson and Mark Hannington is gratefully acknowledged. We thank Kevin Faure for oxygen and hydrogen stable isotope analyses at the Institute of Geological and Nuclear Sciences, New Zealand. Geoscience Australia authors publish with permission of the Chief Executive Officer.

REFERENCES

Barton, M.D., and Johnson, D.A., 2004, Footprints of Fe-oxide(-Cu-Au) systems [ext. abs.]: Centre for Global Metallogeny, University of Western Australia Publication 33, p. 112-116.

Bastrakov, E., Shvarov, Y., Girvan, S., Cleverley, J., and Wyborn, L., 2004, FreeGs: web-enabled thermodynamic database for modeling of geochemical processes [abs]: Australian Geological Convention, 17th, Geological Society of Australia, Abstracts, no. 73, p. 52.

Belperio, A.P., 2002, The Prominent Hill copper-gold discovery: Exploration strategies for world-class iron oxide Cu-Au deposits [abs]: Australian Geological Convention, 16th, Geological Society of Australia, Abstracts, no.67, p. 257.

Campbell, A., Rye, D., and Peterson, U., 1984, A hydrogen and oxygen isotope study of the San Cristobal mine, Peru: Implications of the role of water to rock ratio for the genesis of wolframite deposits: Economic Geology, v. 79, p. 1818–1832.

Clayton, R.N., and Kieffer, S.W., 1991, Oxygen isotopic thermometer calibrations, *in* Taylor, H.P.J., O'Neil, J.R., and Kaplan, I., eds., Stable isotope geochemistry: A tribute to Samuel Epstein: University Park, PA, Geochemical Society, p. 3–10.

Cole, D.R., Horita, J., Polyakov, V.B., Valley, J.W., Spicuzza, M.J., and Coffey, D.W., 2004, An experimental and theoretical determination of oxygen isotope fractionation in the system magnetite-H_2O from 300 to 800°C: Geochimica et Cosmochimica Acta, v. 68, p. 3569–3585.

Conor, C.H.H., 1995, Moonta-Wallaroo region: An interpretation of the geology of the Maitland and Wallaroo 1:100 000 sheet areas: Mines and Energy South Australia Open File Envelope 8886, DME 588/93.

Creaser, R.A., 1989, The geology and petrology of Middle Proterozoic felsic magmatism of the Stuart Shelf, South Australia: Unpublished Ph.D. thesis, Melbourne, La Trobe University, 434 p.

Creaser, R.A., and Cooper, J.A., 1993, U-Pb geochronology of middle Proterozoic felsic magmatism surrounding the Olympic Dam Cu-U-Au-Ag and Moonta Cu-Au-Ag deposits, South Australia: Economic Geology, v. 88, p. 186–197.

Curtis, J.L., Vanderstelt, B.J., and Parker, A.J., 1993, Pre-Adelaidean basement to the Stuart Shelf, South Australia: Drill hole database and preliminary geological interpretation: Department of Mines and Energy, Geological Survey, South Australia, Report Book 93/95, p. 28.

Daly, S.J., Fanning, C.M., and Fairclough, M.C., 1998, Tectonic evolution and exploration potential of the Gawler craton: AGSO Journal of Australian Geology and Geophysics, v. 17, p. 145–168.

Davidson, G.J., and Paterson, H.L., 1993, Oak Dam East: A prodigious, uranium-bearing, massive iron oxide body on the Stuart Shelf [abs.]: Geological Society of Australia Abstracts, v. 34, p. 18–19.

Davidson, G.J., Paterson, H., Meffre, S., and Berry, R.F., 2007, Characteristics and origin of the Oak Dam East breccia-hosted, iron oxide-Cu-U-(Au) deposit: Olympic Dam region, Gawler craton, South Australia: Economic Geology, v. 102, p. 1471–1498.

Direen, N.G., and Lyons, P., 2002, Geophysical interpretation of the central Olympic Cu- Direen, N.G., 2007, Regional crustal setting of iron oxide Cu-Au mineral systems of the Olympic Dam region, South Australia: Insights from potential field modeling: Economic Geology, v. 102, p. 1397–1414.

Drexel, J.F., Preiss, W.V., and Parker, A.J., 1993, The geology of South Australia. Volume 1, The Precambrian: South Australia, Geological Survey Bulletin 54, 242 p.

Eldridge, C.S., and Danti, K., 1994, Low sulfur isotope ratios: High gold values—a closer look at the Olympic Dam deposit via SHRIMP [abs]: Geological Society of America Abstracts with Programs, p. A-498–A-499.

Fontes, J.C., and Matray, J.M., 1993, Geochemistry and origin of formation brines from the Paris basin, France: 1. Brines associated with Triassic salts: Chemical Geology, v. 109, p. 149–175.

Gow, P.A., 1996, Geological evolution of the Stuart Shelf and Proterozoic iron oxide-associated mineralization: Insights from regional geophysical data: Unpublished Ph.D. thesis, Melbourne, Monash University, 151 p.

Gow, P.A., Wall, V.J., Oliver, N.H.S., and Valenta, R.K., 1994, Proterozoic iron oxide (Cu-U-Au-REE) deposits: Further evidence of hydrothermal origins: Geology, v. 22, p. 633–636.

Hampton, S., 1997, A study of the paragenesis and controls on Proterozoic (Cu-Fe-Au-REE) mineralization at the Manxman A1 and Joes Dam South prospects, Mount Woods inlier, South Australia: Unpublished Honours thesis, Townsville, James Cook University of North Queensland, 146 p.

Hand, M., Reid, A., and Jagodzinski, E., 2007, Tectonic framework and evolution of the Gawler craton, Southern Australia: Economic Geology, v. 102, p. 1377–1395.

Haynes, D.W., Cross, K.C., Bills, R.T., and Reed, M.H., 1995, Olympic Dam ore genesis: A fluid-mixing model: Economic Geology, v. 90, p. 281–307.

Heinrich, C.A., Walshe, J.L., and Harrold, B.P., 1996, Chemical mass transfer modeling of ore-forming hydrothermal systems: Current practise and problems: Ore Geology Reviews, v. 10, p. 319–338.

Heinrich, C.A., Driesner, T., Stefansson, A., and Seward, T., 2004, Magmatic vapor contraction and the transport of gold from the porphyry environment to epithermal ore deposits: Geology, v. 32, p. 761–764.

Hitzman, M.W., 2000, Iron oxide-Cu-Au deposits: What, where, when, and why, *in* Porter, T.M., ed., Hydrothermal iron oxide copper-gold and related deposits: A global perspective: Adelaide, Australian Mineral Foundation, v.1, p. 9–25.

Hitzman, M.W., Oreskes, N., and Einaudi, M.T., 1992, Geological characteristics and tectonic setting of Proterozoic iron oxide (Cu-U-Au-REE) deposits: Precambrian Research, v. 58, p. 241–287.

Huston, D.L., Power, M., Gemmell, J.B., and Large, R.R., 1995, Design, calibration and geological application of the first operational Australian Laser ablation sulfur isotope microprobe: Australian Journal of Earth Sciences, v. 42, p. 549–555.

Jagodzinski, E.A., 2005, Compilation of SHRIMP U-Pb geochronological data, Olympic domain, Gawler craton, South Australia: Geoscience Australia, Record 2005/20.

Johnson, J.P., 1993, The geochronology and radiogenic isotope systematics of the Olympic Dam copper-uranium-gold-silver deposit, South Australia: Unpublished Ph.D. thesis, Canberra, Australian National University, 252 p.

Johnson, J.P., and Cross, K.C., 1995, U-Pb geochronological constraints on the genesis of the Olympic Dam Cu-U-Au-Ag deposit, South Australia: Economic Geology, v. 90, p. 1046–1063.

Johnson, J.P., and McCulloch, M.T., 1995, Sources of mineralizing fluids for the Olympic Dam deposit (South Australia): Sm-Nd isotopic constraints: Chemical Geology, v. 121, p. 177–199.

Johnson, L.H., Burgess, R., Turner, G., Milledge, H.J., and Harris, J.W., 2000, Noble gas and halogen geochemistry of mantle fluids: comparison of African and Canadian diamonds: Geochimica et Cosmochimica Acta, v. 64, p. 717–732.

Kendrick, M.A., Burgess, R., Pattrick, R.A.D., and Turner, G., 2001, Noble gas and halogen evidence on the origin of Cu-porphyry mineralizing fluids: Geochimica et Cosmochimica Acta, v. 65, p. 2651–2668.

Knutson, J., Donnelly, T.H., Eadington, P.J., and Tonkin, D.G., 1992, Hydrothermal alteration of middle Proterozoic basalts, Stuart Shelf, South Australia: A possible source for Cu mineralization: Economic Geology, v. 87, p. 1054–1077.

Mark, G., Foster, D.R.W., Pollard, P.J., Williams, P.J., Tolman, J., Darvall, M., and Blake, K.L., 2004, Stable isotope evidence for magmatic fluid input during large-scale Na-Ca alteration in the Cloncurry Fe oxide Cu-Au district, NW Queensland, Australia: Terra Nova, v. 16, p. 54–61.

Matveyeva, S.S., Verkhovsky, A.B., Yurgina, E.K., Shukolyukov, Y.A., Bastrakov, E.N., and Korotayev, M.Y., 1991, Noble-gas and oxygen isotope data on the nature and evolution of the ore-bearing fluids of the Akchatau deposit: Geokhimiya (Geochemistry), no. 3, p. 333–343.

Morales, R.S., Both, R.A., and Golding, S., 2002, A fluid inclusion and stable isotope study of the Moonta copper-gold deposits, South Australia: Evidence for fluid immiscibility in a magmatic hydrothermal system: Chemical Geology, v. 192, p. 211–226.

Mortimer, G.E., Cooper, J.A., Paterson, H.L., Cross, K., Hudson, G.R.T., and Uppill, R.K., 1988, Zircon U-Pb dating in the vicinity of the Olympic Dam Cu-U-Au deposit, Roxby Downs, South Australia: Economic Geology, v. 83, p. 694–709.

Ohmoto, H., 1972, Systematics of sulfur and carbon isotopes in hydrothermal ore deposits: Economic Geology, v. 67, p. 551–578.

——1986, Stable isotope geochemistry of ore deposits: Reviews in Mineralogy, v. 16, p. 491–560.

Oreskes, N., and Einaudi, M.T., 1990, Origin of rare earth element-enriched hematite breccias at the Olympic Dam Cu-U-Au-Ag deposit, Roxby Downs, South Australia: Economic Geology, v. 85, p. 1–28.

——1992, Origin of hydrothermal fluids at Olympic Dam: Preliminary results from fluid inclusions and stable isotopes: Economic Geology, v. 87, p. 64–90.

Paterson, H.L., and Muir, P.M., 1986, Stuart Shelf E.L.1316 (part) partial relinquishment report, Western Mining Corporation Limited, Exploration Division, Unpublished Company Report: South Australia, Department of Mines and Energy Open File Envelope 6562.

Reeve, J.S., Cross, K.C., Smith, R.N., and Oreskes, N., 1990, Olympic Dam copper-uranium-gold-silver deposit: Melbourne, Australasian Institute of Mining and Metallurgy Monograph Series 14, p. 1009–1035.

Reynolds, L.J., 2000, Geology of the Olympic Dam Cu-U-Au-Ag-REE deposit, *in* Porter, T.M., ed., Hydrothermal iron oxide copper-gold and related deposits: A global perspective: Adelaide, Australian Mineral Foundation, v. 1, p. 93–104.

——2001, Geology of the Olympic Dam Cu-U-Au-Ag-REE deposit: MESA Journal, v. 23, p. 4–11.

Robinson, B.W., and Kusabe, M., 1975, Quantitative preparation of SO_2, for $^{34}S/^{32}S$ analyses from sulfides by combustion with cuprous oxide: Analytical Chemistry, v. 47, p. 1179–1181.

Ryan, C.G., Heinrich, C.A., and Mernagh, T.P., 1993, PIXE microanalysis of fluid inclusions and its application to study ore metal segregation between magmatic brine and vapor: Nuclear Instruments and Methods in Physics Research, sec. B. Beam Interactions with Materials and Atoms, v. 77, p. 463–471.

Ryan, C.G., Heinrich, C.A., Van Achterbergh, E., Ballhaus, C., and Mernagh, T.P., 1995, Microanalysis of ore-forming fluids using the scanning proton microprobe: Nuclear Instruments and Methods in Physics Research, sec. B. Beam Interactions with Materials and Atoms, v. 104, p. 182–190.

Sharp, Z.D., 1990, A laser-based microanalytical method for the in situ determination of oxygen isotope ratios of silicates and oxides: Geochimica et Cosmochimica Acta, v. 54, p. 1353–1357.

Shvarov, Y.V., 1999, Algorithmization of the numerical equilibrium modeling of dynamic geochemical processes: Geochemistry International, v. 37, p. 571–576.

Shvarov, Y.V., and Bastrakov, E.N., 1999, HCh: A software package for geochemical equilibrium modeling.User's Guide: Australian Geological Survey Organisation Record 1999/25, 61 p.

Shvarov, Y.V., Borisov, M.V., Grichuk, D.V., and Bastrakov, E.N., 1999, Default UNITHERM database for the HCh package for geochemical modelling: Unpublished computer file available from Geoscience Australia.

Skirrow, R.G., 2000, Gold-copper-bismuth deposits of the Tennant Creek district, Australia: A reappraisal of diverse high-grade systems, *in* Porter, T.M., ed., Hydrothermal iron oxide copper-gold and related deposits: A global perspective: Adelaide, Australian Mineral Foundation, v. 1, p. 149–160.

Skirrow, R.G., Bastrakov, E., Davidson, G., Raymond, O., and Heithersay, P., 2002, The geological framework, distribution and controls of Fe oxide Cu-Au deposits in the Gawler craton. Part II. Alteration and mineralization, South Australia, *in* Porter, T.M., ed., Hydrothermal iron oxide copper-gold and related deposits: A global perspective: Adelaide, Porter GeoConsultancy Publishing, v. 2, p. 33–47.

Skirrow, R.G., Bastrakov, E.N., Barovich, K., Fraser, G.L., Creaser, R.A., Fanning, C.M., Raymond, O.L., and Davidson, G.J., 2007, Timing of iron oxide-Cu-Au(U) hydrothermal activity and Nd isotope constraints on metal sources in the Gawler craton, South Australia: Economic Geology, v. 102, p. 1441–1470.

Taylor, H.P.J., and Sheppard, S.M.F., 1986, Igneous rocks. I. Processes of isotopic fractionation and isotope systematics: Reviews in Mineralogy, v. 16, p. 227-271.

Valley, J.W., 1986, Stable isotope geochemistry of metamorphic rocks, *in* Valley, J.W., Taylor, H.P., and O'Neil, J.R., eds., Stable isotopes in high temperature geological processes: Reviews in Mineralogy, v. 16, p. 445–489.

Vennemann, T.W., and O'Neil, J.R., 1993, A simple and inexpensive method of hydrogen isotope and water analyses of minerals and rocks based on zinc reagent: Chemical Geology, v. 103, p. 227–234.

Williams, P.J., Dong, G., Ryan, C.G., Pollard, P.J., Rotherham, J.F., Mernagh, T.P., and Chapman, L.H., 2001, Geochemistry of hypersaline fluid inclusions from the Starra (Fe oxide)-Au-Cu deposit, Cloncurry district, Queensland: Economic Geology, v. 96, p. 875–883.

Appendix 1

Diamond Drill Holes Examined in the Study, with Observed Alteration Assemblages and their Sequence

Drill hole	Longitude (°)	Latitude (°)	Alteration
ACD 1	136.748883	–30.620644	CAM/HSCC
AD 8	137.123430	–31.095081	CAM/HSCC
ASD 1	137.108857	–31.036490	
ASD 2	137.022249	–31.019981	
BD 1	136.843695	–30.148629	CAM
BDH 3	137.608738	–31.828429	HSCC
BLD 1	137.215711	–30.380225	HSCC
BLD 2	137.263139	–30.412508	
BLD 3	137.320053	–30.375328	
CSD 1	136.844595	–30.949167	CAM/HSCC
DD85EN 17	135.438973	-29.667094	MB
DD85EN 20	135.382864	-29.586494	MB
DD86EN 26	135.348502	-29.652290	MB
DD86EN 33	135.145424	-29.296348	MB
DD89EN 61	135.387832	-29.669962	CAM/HSCC
DRD 1	137.174483	–30.784385	CAM/HSCC
EC 21	137.210072	–31.377512	HSCC
HHD 1	136.769102	–30.782606	
HUD 1	137.342490	–31.179227	HSCC
HWD 1	137.055787	–30.932023	HSCC
MRD 1	137.769346	–30.966366	CAM
NHD 1	137.565153	–31.274311	
PY 3	137.201194	–31.394451	HSCC
PY 4	137.234334	–31.462237	HSCC
SAE4	137.140903	–31.110939	CAM/HSCC
SAE6	137.149384	–31.110437	CAM/HSCC
SAE7	137.116203	–31.126951	CAM
SAR 7	137.448619	–31.608750	HSCC
SAR 8	137.358967	–31.588937	HSCC
SAR 9	137.347823	–31.568101	
SLT 103	137.505138	–31.758017	HSCC
SLT 104	137.696313	–31.911577	
TD 2	137.652617	–30.780404	CAM/HSCC
WRD 1	136.951320	–30.648533	HSCC

Notes: Abbreviations of alteration mineral assemblages: CAM = calc-silicate-alkali feldspar-magnetite, HSCC = hematite-sericite-chlorite-carbonate, MB = magnetite-biotite; CAM/HSCC = CAM assemblage overprinted by HSCC assemblage

Appendix 2

Starting Compositions of Fluids and Rocks Used for Thermodynamic Analysis of Cu-Au Transport and Deposition for the Reduction (a) and Upgrading (b) Models

(a)

Component	Initial fluid	Granite	Units
H_2O	1.00E+00	0.00E+00	kg
SiO_2	0.00E+00	3.00E+02	g
$KAlSi_3O_8$	0.00E+00	3.00E+02	g
$NaAlSi_3O_8$	0.00E+00	3.00E+02	g
$KAl_3Si3O_{12}H_2$	0.00E+00	2.00E+01	g
$Fe_5Al_2Si3O_{18}H_8$	0.00E+00	5.00E+01	g
Fe_3O_4	0.00E+00	2.00E+01	g
FeS_2	0.00E+00	5.00E+00	g
$CuFeS_2$	0.00E+00	5.00E+00	g
$NaCl_{(aq)}$	2.40E+00	0.00E+00	mol

Notes: f_{O_2} is considered an independent variable and set within the range of –34 to –22 log units

(b)

Component	Initial fluid	Gawler Range Volcanics	Proto-ore	Units
H_2O	1.00E+00	0.00E+00	0.00E+00	kg
$NaCl_{(aq)}$	3.00E+00	0.00E+00	0.00E+00	mol
$KCl_{(aq)}$	0.00E+00	0.00E+00	0.00E+00	mol
$O_{2(aq)}$	1.00E-01	0.00E+00	0.00E+00	mol
SiO_2	0.00E+00	2.50E+02	0.00E+00	g
$KAlSi_3O_8$	0.00E+00	3.00E+02	0.00E+00	g
$NaAlSi_3O_8$	0.00E+00	3.00E+02	0.00E+00	g
$CaAl_2Si_2O_8$	0.00E+00	0.00E+00	0.00E+00	g
$KAl_3Si_3O_{12}H_2$	0.00E+00	5.00E+01	0.00E+00	g
$KFe_3AlSi_3O_{12}H_2$	0.00E+00	3.00E+00	0.00E+00	g
$KMg_3AlSi_3O_{12}H_2$	0.00E+00	3.00E+00	0.00E+00	g
Fe_3O_4	0.00E+00	3.00E+01	9.94E+02	g
FeS_2	0.00E+00	1.00E+00	3.00E+00	g
$CuFeS_2$	0.00E+00	0.00E+00	3.00E+00	g
Au	0.00E+00	0.00E+00	1.00E-04	g